THE GEOLOGICAL SOCIETY OF AMERICA®

A non–plate tectonic model for the Eoarchean Isua supracrustal belt

A. Alexander G. Webb[1,*], Thomas Müller[2], Jiawei Zuo[1], Peter J. Haproff[3], and Anthony Ramírez-Salazar[2]
[1]DEPARTMENT OF EARTH SCIENCES AND LABORATORY FOR SPACE RESEARCH, UNIVERSITY OF HONG KONG, POKFULAM ROAD, HONG KONG, CHINA
[2]SCHOOL OF EARTH AND ENVIRONMENT, UNIVERSITY OF LEEDS, MATHS/EARTH AND ENVIRONMENT BUILDING, LEEDS LS2 9JT, UK
[3]DEPARTMENT OF EARTH AND OCEAN SCIENCES, UNIVERSITY OF NORTH CAROLINA, WILMINGTON, NORTH CAROLINA 28403, USA

ABSTRACT

The ca. 3.8–3.6-b.y.-old Isua supracrustal belt of SW Greenland is Earth's only site older than 3.2 Ga that is exclusively interpreted via plate-tectonic theory. The belt is divided into ca. 3.8 Ga and ca. 3.7 Ga halves, and these are interpreted as plate fragments that collided by ca. 3.6 Ga. However, such models are based on idiosyncratic interpretations of field observations and U-Pb zircon data, resulting in intricate, conflicting stratigraphic and structural interpretations. We reanalyzed published geochronological work and associated field constraints previously interpreted to show multiple plate-tectonic events and conducted field-based exploration of metamorphic and structural gradients previously interpreted to show heterogeneities recording plate-tectonic processes. Simpler interpretations are viable, i.e., the belt may have experienced nearly homogeneous metamorphic conditions and strain during a single deformation event prior to intrusion of ca. 3.5 Ga mafic dikes. Curtain and sheath folds occur at multiple scales throughout the belt, with the entire belt potentially representing Earth's largest a-type fold. Integrating these findings, we present a new model in which two cycles of volcanic burial and resultant melting and tonalite-trondhjemite-granodiorite (TTG) intrusion produced first the ca. 3.8 Ga rocks and then the overlying ca. 3.7 Ga rocks, after which the whole belt was deformed and thinned in a shear zone, producing the multiscale a-type folding patterns. The Eoarchean assembly of the Isua supracrustal belt is therefore most simply explained by vertical stacking of volcanic and intrusive rocks followed by a single shearing event. In combination with well-preserved Paleoarchean terranes, these rocks record the waning downward advection of lithosphere inherent in volcanism-dominated heat-pipe tectonic models for early Earth. These interpretations are consistent with recent findings that early crust-mantle dynamics are remarkably similar across the solar system's terrestrial bodies.

LITHOSPHERE; v. 12; no. 1; p. 166–179; GSA Data Repository Item 2020114 | Published online 30 January 2020 https://doi.org/10.1130/L1130.1

INTRODUCTION

The linked questions of how and when plate tectonics initiated, and what preceded plate tectonics, are widely regarded as some of the most significant unsolved problems of solid Earth evolution (e.g., Huntington and Klepeis, 2018; Sleep, 2000; Stern, 2008). Persistence of these basic questions 50 years after the main decade of plate-tectonic discovery is in itself remarkable. In these 50 years, we have acquired detailed knowledge about the active plate-tectonic system as well as rapidly growing understanding of interactions among the solid Earth, the atmosphere, the biosphere, and the hydrosphere (e.g., Bird et al., 2008; Boos and Kuang, 2010; Herman et al., 2013; Hoorn et al., 2010; McKenzie et al., 2016). In contrast to this increasing specificity, viable models of early Earth's tectonics range from plate tectonics emerging almost directly from a magma ocean before 4.4 Ga (e.g., Harrison et al., 2017) to onset of plate tectonics as late as the Neoproterozoic (e.g., Stern et al., 2016).

Uncertainty regarding early tectonics reflects early Earth's sparse geologic record. In contrast to the rich early records of the solar system's other terrestrial bodies, Earth's geologic record is generally more fragmentary the further back in time that it is accessed (Michalski et al., 2018). The incomplete geologic record, with associated preservation bias potential and small numbers statistical issues, limits our ability to conclusively test most relevant models. As the record becomes less complete deeper in time, it generally becomes simpler. Associations of lithologies, distinct rock types, and mineralogy are all reduced in diversity progressively back through time (e.g., Hazen et al., 2008; Stern, 2008). Terrane records from before the Archean-Proterozoic transition are dominated by relatively simple granitoid-greenstone successions (e.g., Condie, 2019). Prior to ca. 3.2 Ga, such successions are the only lithologies observed (e.g., Byerly et al., 2019; Nutman and Bennett, 2019; Van Kranendonk et al., 2019). The eldest kilometer-scale rock packages are granitoid-greenstone terranes developed from ca. 3.85 Ga to ca. 3.7 Ga (e.g., Cates et al., 2013; Nutman and Friend, 2009; O'Neil et al., 2008). For the period before 4.0 Ga, our only record is a granitoid from Acasta of NW Canada (Bowring and Williams, 1999; Reimink et al., 2016) and zircon crystals, predominantly detrital zircon grains principally sourced from just two localities separated by ~100 km in western Australia (Compston and Pidgeon, 1986; Froude et al., 1983; Mojzsis et al., 2001; Wilde et al., 2001).

By interpreting the early Earth record to be at least roughly representative, many workers have used mineralogical (e.g., Hazen et al., 2008; Shirey and Richardson, 2011), geological (e.g., Brown and Johnson, 2018; Pease et al., 2008), and geochemical records (e.g., Johnson et al., 2019; Keller and Schoene, 2012), particularly

Andrew Alexander Gordon Webb http://orcid.org/0000-0001-8007-8489
*Corresponding author: aagwebb@hku.hk

those recorded by fine-grained sediments (e.g., Tang et al., 2016) and zircon crystals (e.g., Dhuime et al., 2012; Næraa et al., 2012), to infer a major shift in Earth's crustal generation processes at ca. 3.2–2.5 Ga. The most common hypothesis to explain this shift is the onset of plate-tectonic recycling following some form of hot stagnant lid geodynamics (e.g., Lenardic, 2018). However, a focus on tectono-metamorphic geology highlights a finding that contradicts this overall interpretation. Namely, all prior detailed geologic studies of our best-preserved Eoarchean terrane, the ca. 3.85–3.60 Ga Isua supracrustal belt of SW Greenland, interpret this site to record terrane collision within the context of plate tectonics (Arai et al., 2015; Hanmer and Greene, 2002; Komiya et al., 1999; Nutman et al., 2015b; Nutman and Friend, 2009). It is worth considering that an individual record of subduction and terrane collision does not require global plate tectonics; for example, proposed Venusian subduction at the Artemis corona is spatially restricted within an otherwise stagnant lid setting (Davaille et al., 2017). Nonetheless, Isua represents a significant counterweight to the assumption underpinning the ca. 3 Ga tectonic-mode-change models, i.e., the idea that early Earth's record is broadly representative.

We speculate that the exclusivity of subduction tectonic interpretations for the Isua supracrustal belt is largely a function of relatively sparse structural study. Although the antiquity and significance of the belt have been recognized since the 1970s (Moorbath et al., 1972; Moorbath et al., 1973), and signal insights into early Earth processes have been derived from Isua since then (e.g., Allwood et al., 2018; Bennett et al., 2007; Cabral et al., 2013; Caro et al., 2003; Crowe et al., 2013; Frei et al., 2016; Hassenkam et al., 2017; Komiya et al., 1999; Moore and Webb, 2013; Næraa et al., 2012; Nutman et al., 2016; Rizo et al., 2012; Rosing et al., 2010), only about 10 research groups have published structural information about the belt (Allwood et al., 2018; Appel et al., 1998; Bridgwater and McGregor, 1974; Crowley, 2003; Crowley et al., 2002; Fedo, 2000; Fedo et al., 2001; Friend and Nutman, 2005, 2010, 2011; Friend et al., 2008; Hanmer and Greene, 2002; Hanmer et al., 2002; James, 1976; Kaczmarek et al., 2016; Keto and Kurki, 1967; Komiya et al., 1999; Kurki and Keto, 1966; Myers, 2001; Nutman, 1984; Nutman and Bennett, 2019; Nutman and Bridgwater, 1986; Nutman and Friend, 2007, 2009; Nutman et al., 1997, 2000, 2002, 2007, 2013, 2015a, 2015b, 2015c, 2015d, 2016, 2019; Rosing et al., 1996), a diversity of interrogations which is greatly surpassed for most other subaerial orogenic belts on Earth. In this contribution, we examined the evidence used to support plate-tectonic interpretations, focusing on (1) reanalysis of prior geochronological results and associated cross-cutting relationships that have previously been interpreted to record as many as eight tectonic events, and (2) new field observations leading to reinterpretation of basic structural relationships. We integrated these findings to explore whether non–plate tectonic models are viable, and indeed might represent simpler interpretations of the available data.

GEOLOGICAL BACKGROUND

The protoliths of Eoarchean Isua rocks match those of all other pre–3.2 Ga terranes: (1) mafic and ultramafic igneous rocks (i.e., basalts, komatiites, and their intrusive equivalents), (2) crystallized melts of such rocks (i.e., the tonalite-trondhjemite-granodiorite [TTG] series), (3) chemical sedimentary rocks (e.g., chert and banded-iron-formation layers), (4) volumetrically minor crystallized melts of felsic crust (i.e., granites), and (5) clastic sedimentary rocks composed of sediment from the aforementioned rock types (Fig. 1; Moyen and Martin, 2012; Nutman et al., 2015c). The exclusively plate-tectonic interpretations of the Isua supracrustal belt record are based on a broad range of evidence, including identification of ophiolites, arc sequences, metamorphic patterns, accretionary prisms, and large-magnitude thrust-tectonic events. Current plate-tectonic interpretations use the juxtaposition of ca. 3.8 Ga and ca. 3.7 Ga stratigraphic sequences and flanking TTG bodies to infer a suture zone and/or accretionary complex along the ~35 km length of the Isua supracrustal belt, with initial collision prior to intrusion of small volumes of ca. 3.66–3.60 Ga granites observed in all rock packages (e.g., Arai et al., 2015; Nutman and Friend, 2009). Despite agreement on an overarching plate-tectonic setting, basic aspects of the geometric, kinematic, and petrologic framework of Isua are disputed. For example, the same supracrustal rocks are interpreted as ophiolites, arc sequences, and an accretionary prism.

Many of the bases for plate-tectonic interpretations have been shown to be nonconclusive, particularly those founded on igneous rock

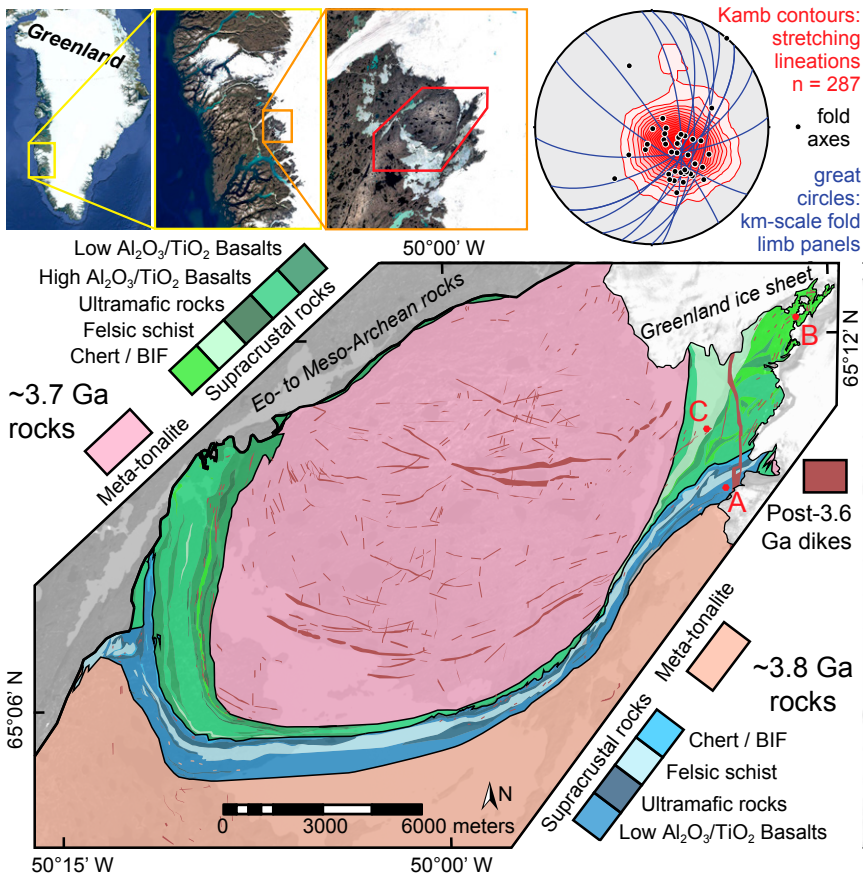

Figure 1. Location, schematic geologic map (modified from Nutman and Friend, 2009), and stereoplot showing key aspects of the Isua supracrustal belt. Red lettered positions on the map correspond to Figure 4 photograph locations. BIF—banded iron formation.

assemblages and/or geochemical constraints: (1) Some workers have deemed the belt to be (in whole or in part) an ophiolite (e.g., Furnes et al., 2007), but subsequent petrological studies preclude this by demonstrating absence and/or misidentification of key components of ophiolite sequences (e.g., Friend and Nutman, 2010). (2) The chemistry of various igneous sequences bears some resemblances to arc magmatic rocks (e.g., Polat and Hofmann, 2003; Polat et al., 2002), but tectonic setting discrimination on this basis is limited by our weak understanding of potential nonuniformitarian geochemical patterns (Bédard et al., 2003; Condie, 2003, 2015). For instance, high Al_2O_3/TiO_2 basalts at Isua have been interpreted to indicate melting in intra-oceanic arc settings (Polat et al., 2002), but similar rocks at Pilbara are interpreted simply as products of remelting of depleted mantle, which can occur in both plate and "vertical" tectonic settings (e.g., partial convective overturn systems, e.g., Smithies et al., 2005). (3) Ultramafic lenses within the belt have been interpreted as mantle slices emplaced in the crust via collisional accretionary faulting (e.g., Kaczmarek et al., 2016), but fractionation trends linking these rocks to adjacent mafic volcanic sequences indicate that these are crustal cumulates (Szilas et al., 2015).

Prior research into the structural framework of the Isua supracrustal belt has posited that the region is dominated by steep southeastward dips and stretching lineations, and that there are fault duplexes, extensive high-magnitude stretching and thinning, and folding (e.g., Hanmer and Greene, 2002; James, 1976; Keto and Kurki, 1967; Komiya et al., 1999; Nutman and Friend, 2009). However, structures are disputed at all scales—even the vergence of proposed subduction is opposite in competing models. One model suggests that the Isua supracrustal belt represents an accretionary prism with hundreds of thrust faults developed over ~100 m.y. via south-dipping subduction (in present coordinates; Fig. 2A; Arai et al., 2015; Komiya et al., 1999). Late extrusion is speculated to have exposed a cross section through the prism, such that peak metamorphic grade decreases from amphibolite to greenschist facies northeastward across the northeastern portion of the belt (Arai et al., 2015; Komiya et al., 1999). The main competing model argues that north-dipping subduction resulted in the ca. 3.69–3.66 Ga collision of ca. 3.8 Ga and ca. 3.7 Ga arc terranes (Fig. 2B; Nutman and Friend, 2009). In this model, deformation was focused along a major suturing shear zone and other shear zones that record distinct events with opposing top-to-the-SE and top-to-the-NW shear senses (Nutman et al., 2015b; Nutman and Friend, 2009). The shear zones are interpreted to separate low-strain zones where facing indicators are locally preserved (Nutman et al., 2015b; Nutman and Friend, 2009).

MODELS OF PLATE TECTONICS FOR THE ISUA SUPRACRUSTAL BELT WITH OPPOSITE SUBDUCTION VERGENCE

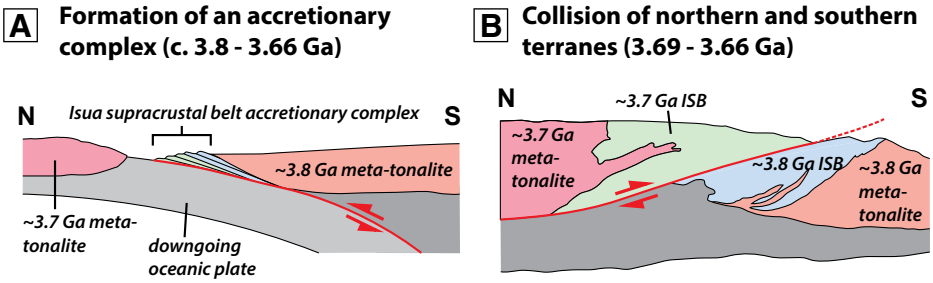

Figure 2. Plate-tectonic models for the Eoarchean assembly of the Isua supracrustal belt: (A) formation of an accretionary prism during south-dipping subduction (modified from Arai et al., 2015), and (B) terrane accretion along a north-dipping subduction zone (modified from Nutman and Friend, 2009). ISB—Isua supracrustal belt.

UTILITY OF EXTANT GEOCHRONOLOGY AND ASSOCIATED FIELD OBSERVATIONS IN RESOLVING DEFORMATION EVENTS

The synthesis of Isua geology that supports the north-dipping subduction model includes multiple distinct Eoarchean deformation events (e.g., Friend and Nutman, 2010; Nutman et al., 2009, 2015b; Nutman and Friend, 2009). In this section, the U-Pb zircon geochronology and associated field observations used to infer these events are reviewed. Unless otherwise noted, all ages are sensitive high-resolution ion microprobe (SHRIMP) U-Pb zircon spot ages. We found that many published tectonic interpretations are permissible, but not required, due to nonunique interpretations of field observations and insufficient geochronological resolution in the face of challenges such as Pb loss (e.g., Fisher and Vervoort, 2018). Furthermore, an interpretation with only a single significant Eoarchean deformation event at Isua is equally viable. This section concludes with a brief review of metamorphic timing constraints from mineral-isotope systems beyond U-Pb zircon.

Before examining the evidence for each proposed deformation event, we affirm other key discoveries provided by U-Pb zircon geochronology at Isua: (1) The division of the Isua supracrustal belt into a northern ca. 3.7 Ga belt and a southern ca. 3.8 Ga belt is robust. This is illustrated via a compilation of SHRIMP U-Pb zircon spot ages from meta-tonalites and felsic metavolcanics in the Isua area from Nutman et al. (2013); see Figure 3A. The distribution of ages clearly shows peaks at ca. 3.7 Ga and ca. 3.8 Ga, and the geographic division between samples that yield the different ages is well established (e.g., Crowley, 2003; Crowley et al., 2002; Nutman et al., 1997, 2009). The ages comprising each peak span 40–50 m.y. intervals. The ~100 m.y. age division illustrated here is a key component of every viable model for Isua, and the main basis for the interpretation that a ca. 3.8 Ga arc subducted northward below and collided with a ca. 3.7 Ga arc. (2) An ~50-m-thick sedimentary layer dominated by chert and banded iron formation occurring discontinuously along the boundary of the ca. 3.7 Ga and ca. 3.8 Ga belts has thus far only yielded 29 U-Pb zircon analyses on 19 grains from three samples (Nutman et al., 2009). Nonetheless, the age distributions are sufficiently well resolved to indicate that this layer received detritus that is distinct from the materials dominating the ca. 3.7 Ga and ca. 3.8 Ga belts. Data from five grains cluster to suggest an age peak at ca. 3.76 Ga, data from 12 grains cluster to suggest a broad age peak spanning from ca. 3.93 Ga to ca. 3.87 Ga, and only a single grain's data are generally consistent with the ca. 3.8 Ga peak (Nutman et al., 2009). (3) All major tectonic events directly disrupting the continuity of Isua rocks are generally understood to have been completed by ca. 3.5 Ga, because intrusion of mafic dikes occurred across the region at that time, and these dikes remain weakly deformed to undeformed (e.g., Nutman et al., 2004; see Fig. 1 herein).

In addition to the proposed collision of ca. 3.8 Ga and ca. 3.7 Ga terranes, up to six more Eoarchean tectonic events have been associated with the north-dipping subduction model (e.g., Friend et al., 2002; Nutman et al., 2015b; Nutman and Friend, 2009). The oldest of the proposed Eoarchean events would have occurred prior to, or at, 3.8 Ga. Friend et al. (2002) stated that, within an ~100-m-long enclave surrounded by 3.8 Ga meta-tonalite, (1) mylonites separate

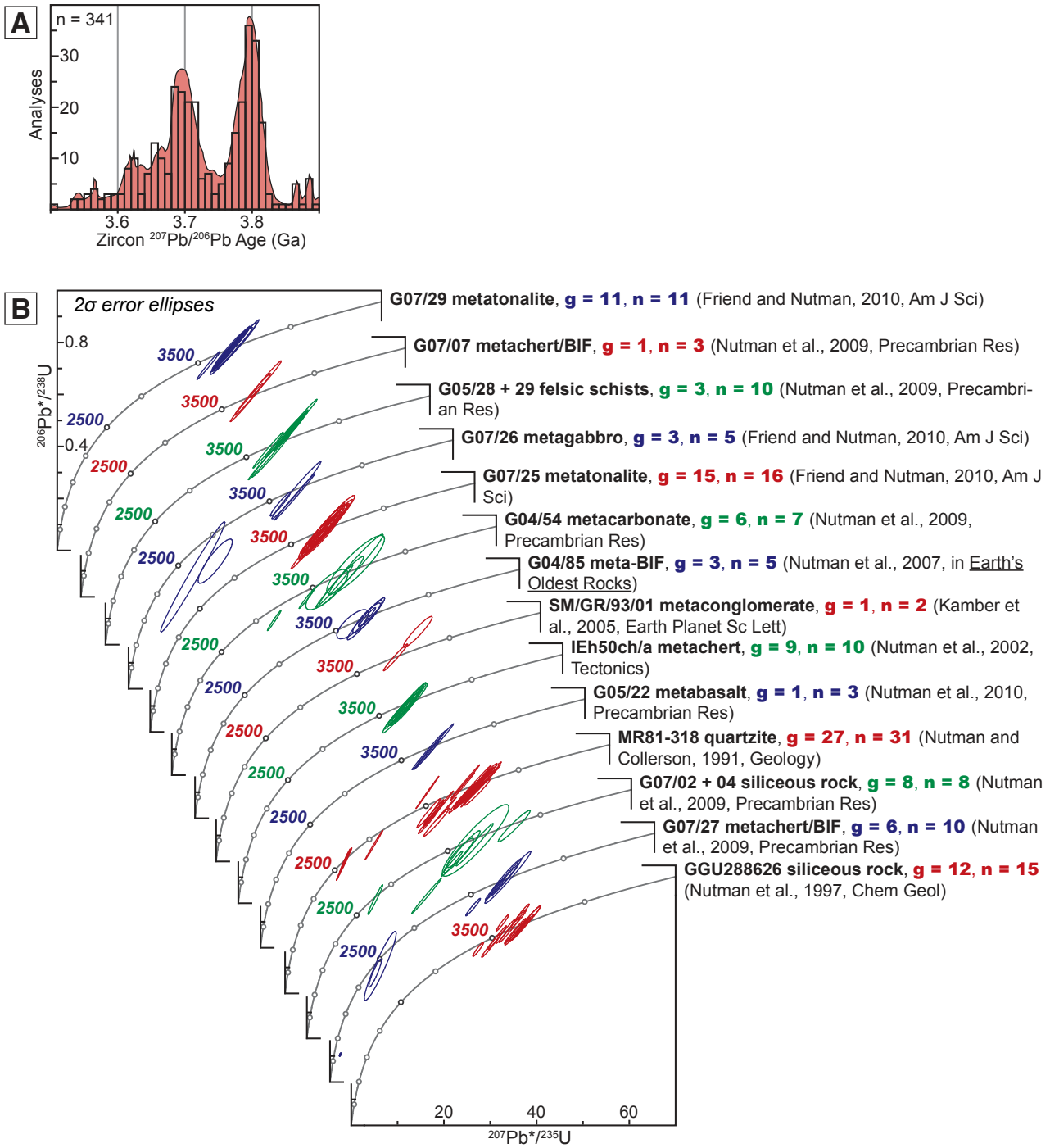

Figure 3. Selected sensitive high-resolution ion microprobe (SHRIMP) U-Pb zircon geochronology constraints relevant to interpretations of the Eoarchean tectonics of the Isua supracrustal belt (see text for details). (A) Histogram and relative probability of zircon ages from meta-tonalite and felsic schist samples of the Isua region, from Nutman et al. (2013). (B) Data proposed to constrain deformation events across Isua shown in traditional concordia plots. Letters "g" and "n" refer to number of dated zircon crystals/detrital grains and number of spot analyses, respectively. Blue, red, and green color coding allows for visual distinction of data plotted on different, closely spaced concordia curves. (C) Traditional concordia plots highlighting the Eoarchean through Paleoarchean time period, with the same data and plotting approach as in part B. (D) Selected data proposed to constrain deformation events across Isua, with the $^{207}Pb/^{206}Pb$ dates for each spot analysis shown with 2σ error bars. Colors and letters ("g" and "n") are used as in part B. (E) Histogram and relative probability of detrital zircon results for four samples from a metasedimentary layer in northeastern Isua (G04/54 *in* Nutman et al., 2009; G04/85 *in* Nutman et al., 2007; IEh50ch *in* Nutman et al., 2009; SM/GR/93/01 *in* Kamber et al., 2005). BIF—banded iron formation. (*Continued on following two pages.*)

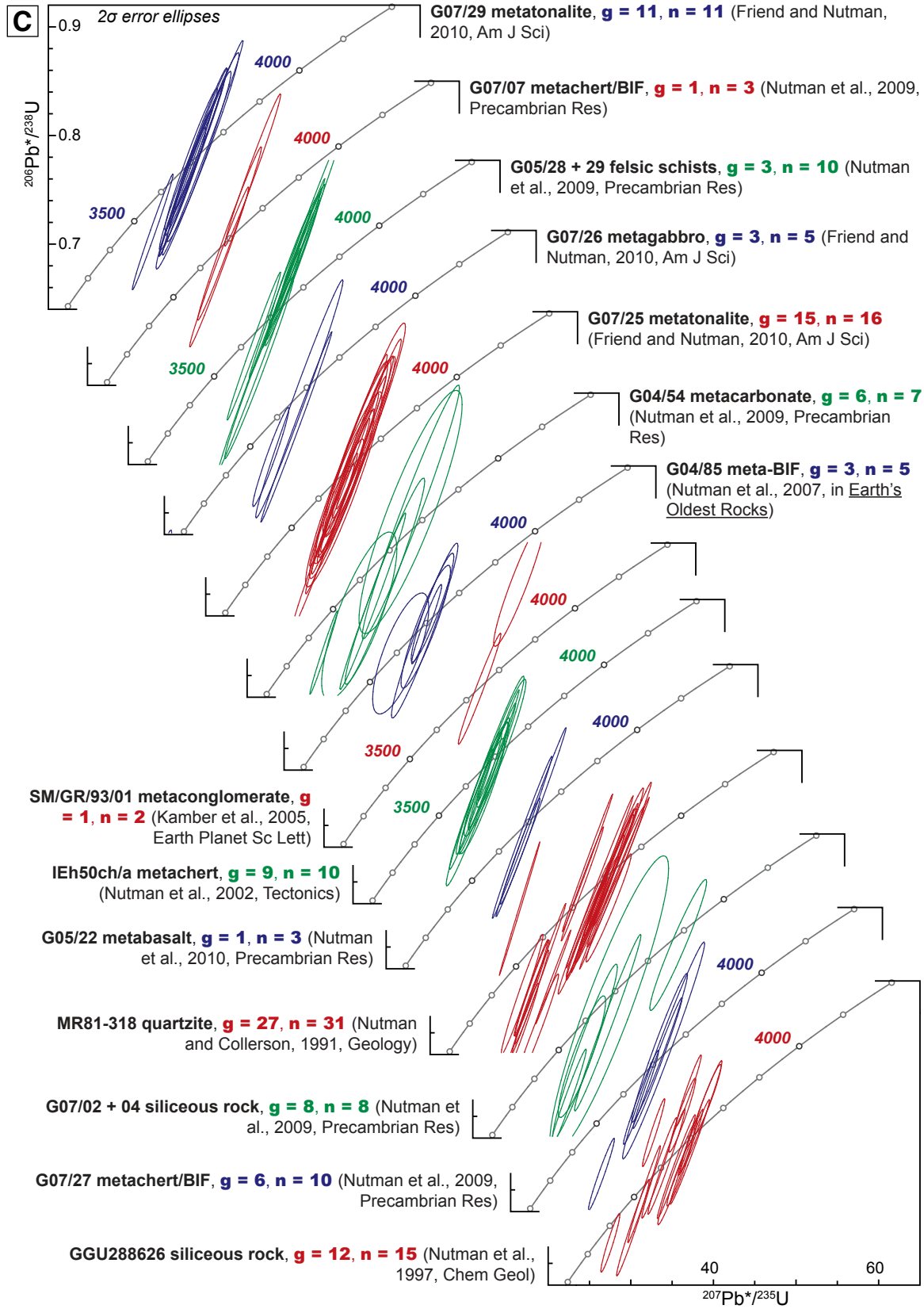

Figure 3 (*continued*).

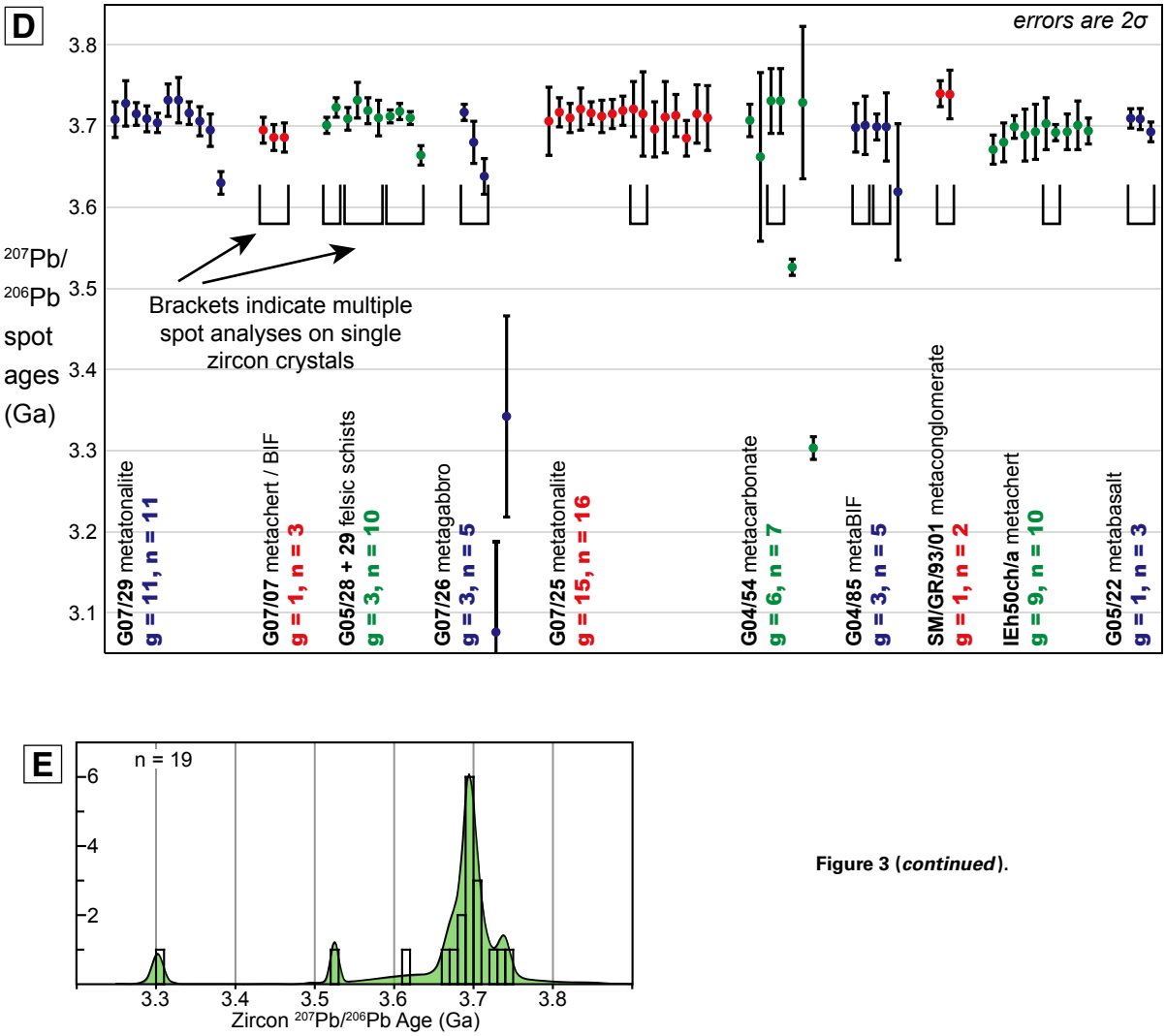

Figure 3 (*continued*).

dunite from layered mafic/ultramafic rocks and (2) relict igneous textures in meta-gabbroic rocks are crosscut along this contact. They interpreted the dunite as mantle rock and the contact as a major fault. However, dunite is a common crustal cumulate rock in granite-greenstone belts (e.g., Szilas et al., 2015). Therefore, tectonic emplacement of mantle material (Nutman et al., 2013) is a nonunique interpretation, and the large shear magnitudes inherent in this model are not required.

The second oldest proposed Eoarchean tectonic event involves a similar geometric framework, with tectonically juxtaposed mafic and ultramafic rocks crosscut by a later tonalitic intrusion, such that the age of the meta-tonalite represents a minimum age for the earlier deformation. Friend and Nutman (2010) stated that ultramafic schist and high Al_2O_3/TiO_2 amphibolite are interspersed in a deformed zone (near the eastern margin of the ca. 3.7 Ga portion of the western part of the Isua supracrustal belt). They showed a photograph (their fig. 3C) that they described as showing nearby, "less deformed" quartz diorite/tonalite crosscutting fabric in the amphibolite. It is difficult to confirm this observation using the photograph because of the lichen cover and washed-out white color of the tonalite rock; the tonalite simply appears in sheets with indeterminate internal morphologies concordant with probable foliation in the basaltic schists. Friend and Nutman (2010) sampled this tonalite (sample G07/29) and obtained 11 SHRIMP U-Pb zircon spot ages from 11 zircon crystals (their fig. 4C and table 2; our Figs. 3B–3D). For the best age of the tonalite, they reported 3717 ± 6 Ma (2σ) as a weighted mean of 9 of the 11 ^{207}Pb/^{206}Pb spot ages; the nine ages are reported as "indistinguishable." We were unable to determine which nine ages were used because: (1) at the 1σ threshold reported in their table 2, fewer than nine ^{207}Pb/^{206}Pb ages overlap, whereas at 2σ, all ages but one age overlap, and (2) we could not reproduce precisely this weighted mean age from any combination of nine ^{207}Pb/^{206}Pb spot ages. Exclusion of the youngest two ages (in order to skew the weighted mean age toward the oldest possibility) yielded a weighted mean of 3713.2 ± 5.7 Ma (2σ), with mean square of weighted deviates (MSWD) = 1.3 and probability of fit = 0.25; exclusion of only the youngest age yielded a weighted mean of 3711.9 ± 5.4 Ma (2σ) with MSWD = 1.5 and probability of fit = 0.15; and inclusion of all ages yielded a weighted mean of 3701 ± 21 Ma (95% confidence) with MSWD = 13 and probability of fit = 0.00 (all results obtained via Isoplot [Ludwig, 2012] and confirmed via calculation). The "probability of fit" refers to the probability that the errors for each individual analysis (i.e., each spot age) will have at least the observed amount of scatter (Ludwig, 2012). The calculations suggest that for this data set, these probabilities are low. Considering this, as well as the small number of analyses, these errors are best considered as a minimum estimate of the true errors (Ludwig,

2012). Therefore, even after excluding outliers, the analytical errors may not capture the actual uncertainty of the tonalite crystallization age. For example, geological error such as complications due to multiple Pb loss events could impact the age scatter. Therefore, a broader view is viable: The results appear to fit well within the broad distribution of the ca. 3.7 Ga age peak from the Nutman et al. (2013) compilation (Fig. 3A). In summary, there is insufficient evidence to be certain of the key crosscutting relationship, and a conservative evaluation of the geochronological data assigns these results to the ca. 3.7 Ga age peak.

Three deformation events have been proposed in time windows that overlap with the ca. 3.69–3.66 Ga period in which north-dipping subduction and collision juxtaposing the two main sequences are posited (e.g., Nutman et al., 2013, 2015b; Nutman and Friend, 2009). First, in the northwestern part of the Isua supracrustal belt, a panel of metamorphosed banded iron formation interlayered with felsic schists, all of which are sheared, is interpreted as being tectonically emplaced (Nutman et al., 2015b). The rationale for a tectonic juxtaposition is largely geochronologic: The banded iron formation is taken as a younger rock (ca. 3690 Ma) emplaced within a sequence of older felsic schists (3724–3712 Ma), and thus the tectonic juxtaposition would need to be younger than the banded iron formation. Specifically, a sample of the banded iron formation (G07/07, Nutman et al., 2009, their table 1; our Figs. 3B–3D) yielded three spot ages from one zircon crystal for an interpreted maximum depositional age of ca. 3690 Ma, whereas the felsic schists yielded 10 spot ages from three zircon crystals from two directly adjacent samples (G05/28 + /29, Nutman et al., 2009, their table 1; our Figs. 3B–3D). The 3724–3712 Ma ages may inform the crystallization age or the maximum depositional age of the felsic schist protolith, because it is unclear whether the protolith was volcanic or a volcaniclastic sedimentary rock (Nutman et al., 2009). In the latter case, the protoliths of the metamorphosed banded iron formation and felsic schist could have been deposited in sequence. Also, it is important to note that the 3724–3712 Ma range was determined by Nutman et al. (2009) by not including younger spot ages obtained from each crystal because these ages were interpreted to reflect Pb loss. These ages do not appear markedly different in their discordance from older analyses, so geological reasons for the spread in ages could include U loss or inheritance, in which case, the younger ages would be more likely to indicate the crystallization timing (e.g., Faure, 1986). Textural setting cannot explain the age distinctions because many of the different ages come from duplicate SHRIMP spot ages, which analyzed the same spot a second time after repolishing (Nutman et al., 2009). Furthermore, we note that all but the youngest one of these ages fit within the broad ca. 3.7 Ga age peak. In summary, the analyses came from a small number of zircon crystals (only four), and the interpreted age difference between samples G07/07 and G05/28 + /29 is the only constraint indicating a large displacement here. If this possible age difference is alternatively considered insignificant, net displacement could be modest.

In the second deformation event proposed for the ca. 3.69–3.66 Ga period, the whole panel of banded iron formation and felsic schist described directly above (including samples G07/07 and G05/28 + /29) is interpreted as a fault-emplaced slice within high Al_2O_3/TiO_2 amphibolite (Nutman et al., 2015b). Again, the rationale for the proposed tectonism is largely geochronologic: the published interpretation of the first rock panel holds that it was assembled after ca. 3690 Ma, whereas it occurs amidst amphibolite with an interpreted best age of 3717 ± 11 Ma (2σ) or older, so the age difference would suggest tectonic juxtaposition after ca. 3690 Ma. The interpreted best age for the amphibolite is the single oldest $^{207}Pb/^{206}Pb$ spot age measured among five spot ages from three zircon crystals of meta-leucogabbro sample G07/26 (the gabbro protolith is interpreted as a minor lithologic component within, and perhaps intruding, the pillow basalt protolith of the amphibolite stack; Friend and Nutman, 2010). The upper-intercept age for a discordia line calculated with all five ages is also ca. 3717 Ma, but with a fivefold larger error. A nearby portion of the amphibolite pile is also locally crosscut by a 1-m-thick meta-tonalitic dike; this dike is dated at 3712 ± 6 Ma (2σ, weighted mean age) via 16 spot ages on 15 zircon crystals from sample G07/25 (Friend and Nutman, 2010). All age constraints fit within the ca. 3.7 Ga age peak of Nutman et al. (2013; see Figs. 3A and 3D herein). Therefore, these data can also be interpreted to represent sequential deposition of various protoliths, without tectonism.

A third similar deformation event proposed for the ca. 3.69–3.66 Ga period has been inferred in northeastern Isua (Friend et al., 2008; Nutman et al., 2007, 2015b). Here, high Al_2O_3/TiO_2 amphibolite, a meta-sedimentary layer (including chert, banded iron formation, and sparse carbonate), and low Al_2O_3/TiO_2 amphibolite form a layered stack that is deformed in folds with bull's-eye map patterns (e.g., Nutman and Friend, 2009; see Fig. 1 herein; see also GSA Data Repository Fig. DR1[1]). Potential right-way-up indicators such as proposed stromatolites suggest that the low Al_2O_3/TiO_2 amphibolite represents the structurally lowest unit, and the high Al_2O_3/TiO_2 amphibolite represents the top of the stack (Nutman et al., 2016). The age of the low Al_2O_3/TiO_2 amphibolite is interpreted to be 3709 ± 9 Ma (2σ); this is a weighted mean age of the oldest two $^{207}Pb/^{206}Pb$ spot dates of three spot dates on one zircon crystal from meta-basalt sample G05/22 of Nutman et al. (2010; their table R1; our Fig. 3). The age of the metasedimentary sequence is constrained by 24 spot ages on 19 detrital zircon grains from four samples (G04/54 *in* Nutman et al., 2009; G04/85 *in* Nutman et al., 2007; IEh50ch *in* Nutman et al., 2009; SM/GR/93/01 *in* Kamber et al., 2005). The individual $^{207}Pb/^{206}Pb$ spot ages range from 3740 ± 8 Ma (1σ) to 3303 ± 7 Ma (1σ), and grains with multiple spot analyses yielded results within 1σ error overlap ranges (see review by Nutman et al., 2009). The age of the metasedimentary sequence was taken to be ca. 3690 Ma (Nutman et al., 2009, 2015b), consistent with the only significant peak in the relative probability spectra for all 19 detrital zircon grains (taking weighted mean ages for multiply dated grains; Fig. 3E). The high Al_2O_3/TiO_2 amphibolite has not been dated; its age is assumed to match that of high Al_2O_3/TiO_2 amphibolite in the western portion of the Isua supracrustal belt, i.e., ≥ 3717 Ma (see earlier discussion of sample G07/29 in this section). Therefore, the published interpretations have indicated that older high Al_2O_3/TiO_2 amphibolite is emplaced atop younger rocks along a thrust contact (Friend et al., 2008; Nutman et al., 2007, 2015b). However, the age control is sparse, and all ages arguably fit the ca. 3.7 Ga peak, so the data do not preclude the possibility of contiguous sections.

Extensional shearing during ca. 3.66 Ga to ca. 3.61 Ga has been proposed based on U-Pb zircon and titanite geochronology of meter-scale granitic intrusions (e.g., Crowley et al., 2002; Nutman et al., 2013). The intrusions are largely pre- and/or syndeformational (Crowley et al., 2002; Nutman et al., 1996, 2000, 2002, 2013), with proposed postdeformational sheets having relatively young ages (Crowley et al., 2002; Friend et al., 2002; Nutman et al., 2002). The interpretation that deformation was extensional

[1]GSA Data Repository Item 2020114, which contains additional photographs of key geological relationships across the Isua supracrustal belt, as well as a schematic geologic map of the belt (modified from text Fig. 1) showing the distribution of shear-sense indicators observed during our field work and the locations of the data repository photographs, is available at http://www.geosociety.org/datarepository/2020, or on request from editing@geosociety.org.

is based on sparse reports (without orientation information) of outcrop-scale structures such as "sigmoid shapes" and fracture networks (Nutman et al., 2013). However, such features are also common in contractional environments, where they are associated with general shear and intrusion, respectively (e.g., Inger and Harris, 1993; Webb et al., 2011). Therefore, while it is clear that deformation postdated at least some fraction of the ca. 3.66 Ga to ca. 3.61 Ga period, this deformation was not necessarily extensional.

One to four post-Eoarchean tectonic events have been tentatively speculated to have intercalated younger rocks into the Isua supracrustal belt without fundamentally altering the belt geometry (Nutman et al., 2009). Metasedimentary samples from four sites, two in the ca. 3.8 Ga supracrustal sequence (G07/02 + 04, MR81–318) and two in the ca. 3.7 Ga supracrustal sequence (G07/27, GGU288626), yielded detrital zircon ages younger than 3.66 Ga, and as young as ca. 2.5 Ga (Figs. 3B and 3C; Nutman et al., 1997, 2009; Nutman and Collerson, 1991). Tectonism has been cautiously considered as a possible explanation for emplacement of rocks with younger ages within the Isua supracrustal belt (Nutman et al., 2009), but this is difficult to envision given the absence of other indications of large-scale translation and disruption across the belt after ca. 2.5 Ga. Alternatively, Pb loss can account for the young ages.

Geochronology of mineral-isotope systems other than U-Pb zircon is relatively sparse and generally constrains post-Eoarchean static metamorphism and/or cooling, but Sm-Nd garnet geochronologic data have been interpreted to record Eoarchean static metamorphism. There is general agreement that the belt experienced two major medium- to high-temperature metamorphic events: (1) an Eoarchean syntectonic metamorphism, which developed concurrently with observed foliations and lineations in the belt, with a minimum age of ca. 3.5 Ga determined via dates of the weakly deformed Ameralik dikes intruding the belt (Nutman et al., 2004); and (2) an apparently static Neoarchean event recognized in posttectonic garnet rims (Rollinson, 2002, 2003) and lower-amphibolite-facies assemblages overprinting the igneous fabrics of the Ameralik dikes (Nutman et al., 2004, 2013). However, Blichert-Toft and Frei (2001) interpreted an Sm-Nd garnet isochron age of 3714 ± 24 Ma for posttectonic garnets in ca. 3.8 Ga supracrustal rocks. This date conflicts with the findings noted above, i.e., that ca. 3.66 Ga to ca. 3.61 Ga granitic intrusions (dated via U-Pb zircon and titanite geochronology) are largely pre- and/or syndeformational (Crowley et al., 2002; Nutman et al., 1996, 2000, 2002, 2013), with potentially postdeformational sheets having relatively young ages (Crowley et al., 2002; Friend et al., 2002; Nutman et al., 2002). The assumption underpinning the Sm-Nd garnet isochron age may be in error, because the age was derived from garnets from a subset of four samples that were assumed to have equilibrated via a homogeneous fluid that affected the entire belt, such that their isotopic composition would have evolved from the same initial ratio (Blichert-Toft and Frei, 2001). The −14 initial ε_{Nd} value that Blichert-Toft and Frei (2001) calculated for the homogeneous fluid suggests an early differentiated crust, in contrast to isotopic studies showing that the tonalites are primary, nearly noncontaminated melts with (super)chondritic Nd values (e.g., Hoffmann et al., 2014; Gardiner et al., 2019), i.e., of a primary crust. Additional potential metamorphic age constraints include: (1) ca. 3.6 Ga U-Pb ages of titanite in the northern 3.7 Ga tonalites, which may reflect cooling or metamorphism (Crowley et al., 2002); (2) a ca. 2.8 Ga Lu-Hf isochron age of posttectonic garnets from supracrustal rocks, primarily from the 3.8 Ga supracrustal rocks (Blichert-Toft and Frei, 2001); and (3) a ca. 2.8 Ga Sm-Nd isochron age of 3.8 Ga meta-basalt, with the isotopic budget largely controlled by secondary allanite (Frei et al., 2002).

FIELD-BASED METAMORPHIC AND STRUCTURAL OBSERVATIONS

We conducted field exploration of the Isua supracrustal belt, with logistical constraints limiting most of our observations to the northeastern portion of the belt. Although the main thrust of our work was a sampling campaign in support of future analytical studies, our field-based observations centered on metamorphic grade variability and strain concentration in terms of shear sense, magnitude, and structural style. These foci were chosen because metamorphic and strain evidence has been variously interpreted in support of the different plate-tectonic models for the development of the Isua supracrustal belt. Models in which the supracrustal belt represents an accretionary prism developed along a south-dipping subduction zone (Fig. 2B) include testable predictions of (1) a northeastward decrease in prograde metamorphic conditions experienced across the northeastern portion of the belt, from amphibolite facies to greenschist facies (e.g., Arai et al., 2015; Komiya et al., 1999), and (2) dominant top-to-the-north shearing along discrete thrust faults, potentially including a structurally high, thrust-parallel, top-to-the-south normal fault system accommodating wedge extrusion (a la Chemenda et al., 1995). Models in which the belt records the collision and underthrusting of a ca. 3.8 Ga proto-arc beneath a ca. 3.7 Ga proto-arc (Fig. 2A) include testable predictions of (1) strain concentrations along major shear zones and patches of distinctly low strain in which primary structures are preferentially preserved, and (2) complex multiphase deformation including early isoclinal folds and multiple layer-emplacement/interleaving events along various thrust and extensional shear zones (e.g., Nutman et al., 2002, 2015c; Nutman and Friend, 2009). By exploring the field evidence related to these predictions, we could examine the viability and uniqueness of each model.

The supracrustal protolith lithologies observed are consistent with earlier studies (e.g., Komiya et al., 1999; Nutman and Friend, 2009): ultramafic and mafic igneous rocks, including pillow volcanics (Fig. 4A; Data Repository Figs. DR1 and DR2A); felsic volcanic and/or volcaniclastic rocks; and chert, banded iron formation, and minor carbonates. However, our field observations contradict prior work asserting that prograde metamorphism dominates and prograde conditions decrease from amphibolite facies in the southwest to greenschist facies in the far northeast, as recorded by mineralogical changes such as the absence of garnet in the far northeast (Arai et al., 2015; Hayashi et al., 2000; Komiya et al., 1999). We found exposures of garnet in the far northeast (Fig. 4B; Data Repository Figs. DR2B and DR2C), suggesting that roughly consistent prograde amphibolite-facies metamorphism was experienced by the entire belt. Furthermore, we observed that the intensity and extent of retrograde metasomatic alteration increase toward the northeast, as recorded by increasing density of quartz-calcite veining and associated alteration in that area (Fig. DR2D). These veins clearly crosscut the foliation (Fig. DR2C), and the samples associated with them show low-temperature retrogression. Petrographic analysis of the samples revealed late chlorite crosscutting and mimicking the foliation via the chloritization of mafic minerals (Fig. 4C; Fig. DR2C). This would suggest that the strongly foliated chlorite reported in the low- and medium-low-temperature zones of the belt (Arai et al., 2015) might not be representative of the peak metamorphism, but rather a product of late low-temperature overprinting. Therefore, proposed decreases in prograde metamorphic facies in the northeasternmost region may instead reflect increased intensity of retrogression.

Across contacts previously proposed to represent mylonitic shear zones concentrating strain, we observed that lithologies display similar structural and metamorphic patterns (Fig. DR2E). Areas previously proposed to preserve low strain, such as sites where deformed pillow lavas can be observed, show the same

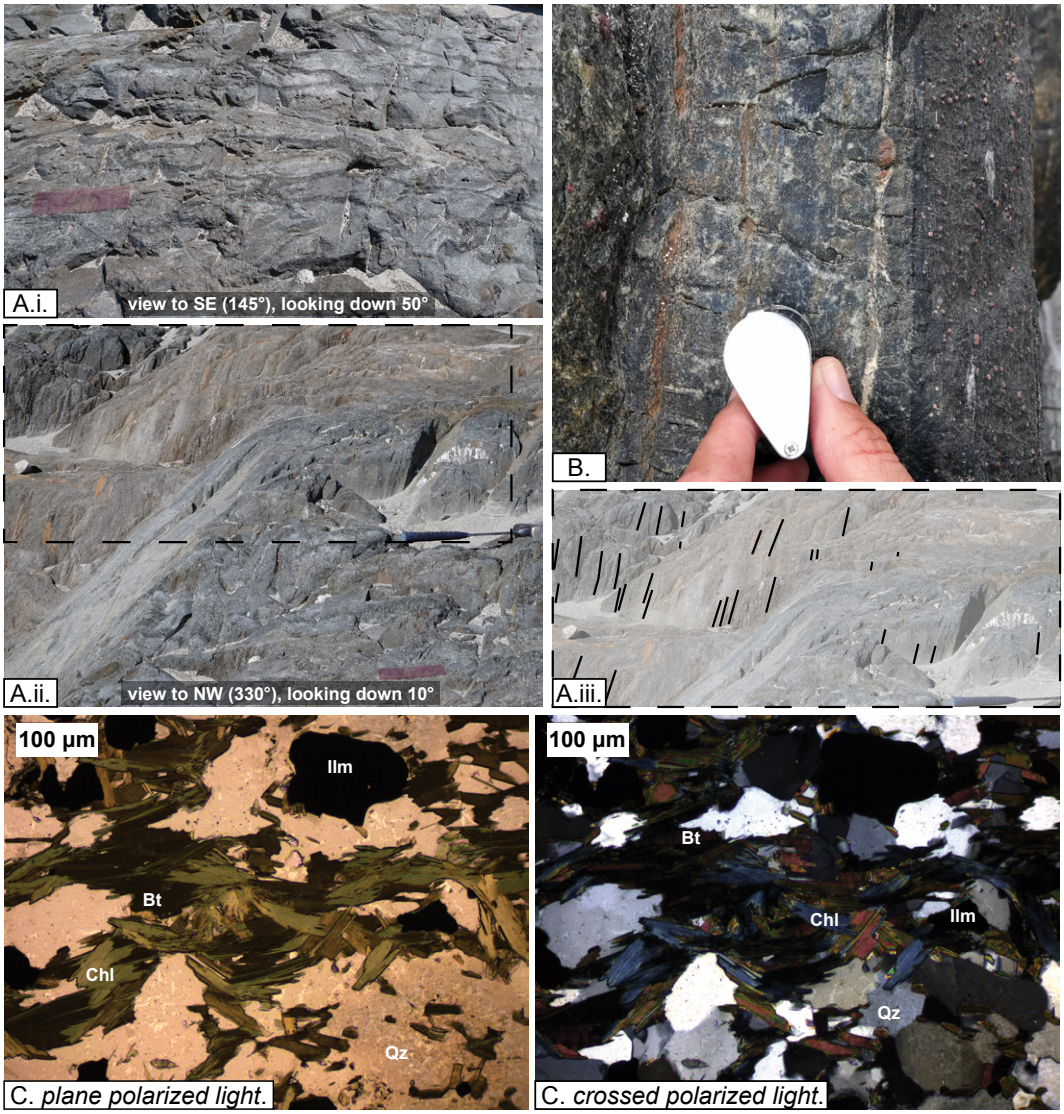

Figure 4. Key structural and metamorphic observations along the northeastern Isua supracrustal belt. Photograph locations are noted in Figure 1. (A) Metamorphosed and strained pillow lavas do not preserve significantly lower strain versus the bulk of the belt; the same penetrative lineation pervades the belt. View (i) looks down the lineation direction, with dark ellipses marking the metamorphosed rims of pillows (6 in. [15 cm] red-tinted ruler for scale). View (ii) looks perpendicular to the foliation and lineation (6 in. [15 cm] red-tinted ruler for scale, in the same location as in part i.). Annotated inset (iii) highlights the lineation visible in (ii). (B) Garnet-bearing mafic schists occur in the far northeastern part of the Isua supracrustal belt, demonstrating that amphibolite-facies prograde conditions were experienced by the entire belt (hand lens for scale). Red garnets occur in layers in the left and right thirds of the image. (C) Chlorite crosscutting biotite in garnet-bearing mafic schists of the northeastern Isua supracrustal belt, indicating retrogression.

foliations and intense stretching lineations as elsewhere (Fig. 4A; Figs. DR2A and DR2F). Therefore, in contrast to prior interpretations, we consider it viable that overall strain is nearly uniform across the supracrustal belt. A recent dialectic over postulated preservation of stromatolites at Isua confirms that primary structures can be only locally preserved in detectable form even within a quasi-uniform overall strain field, due to such aspects as fold-nose preservation and the need for observation surfaces perpendicular to lineation (see Allwood et al., 2018; Nutman et al., 2016, 2019).

Consistent with previous observations (e.g., Hanmer and Greene, 2002; Komiya et al., 1999), both top-to-the-NW shearing and top-to-the-SE shearing were observed without a systematic spatial distribution at kilometer scale (Figs. DR1 and DR2G). Outcrop-scale sheath and curtain folds (i.e., a-type folds, with fold axes parallel to the regional stretching lineation, Fig. 1) are common (Figs. DR2F and DR2H) and may be representative of larger-scale structural patterns. (Sheath folds are so named because they resemble the elongated sheath for a sword. Sheath folds can feature consistent or opposite shear sense indicators in opposing limbs, and these and other a-type folds are generally, but not exclusively, indicative of high strain. For more information and visualizations, see Alsop and Holdsworth [2012] and Wex et al. [2014].) Kilometer-scale folds in northeastern Isua (Nutman and Friend, 2009) show bull's-eye patterns consistent with sheath folding (Fig. DR1). To test whether the entire supracrustal belt may share a similar a-type fold geometry, we determined the dominant foliations of each portion of the belt in ~3 km increments, as taken from our data and published maps (Keto and Kurki, 1967; Nutman and Friend, 2009). These orientations of the kilometer-scale rock panels that define the curves of the Isua supracrustal belt intersect in stereographic projection space along a line parallel to the regional stretching lineation, consistent with an interpretation that the entire belt represents a curtain fold with the intersection line as the fold axis (Fig. 1; Fig. DR1). Observations of outcrop-scale discrete faults (Komiya et al., 1999; see also Fig. DR2F here) and multiple shear senses (Figs. DR1 and DR2G) can likewise be interpreted as components within a-type fold development (e.g., cf. Alsop and Holdsworth, 2012; Cobbold and Quinquis, 1980; Wex et al., 2014). The amplitude and wavelength of the folded Isua supracrustal belt are at the 10^4 m scale. Therefore, if the belt does represent an a-type fold, it is likely the largest a-type fold exposed on Earth, with concomitant implications for the thickness and strain distribution of the early lithosphere.

NEW MODEL FOR THE ASSEMBLY AND DEFORMATION OF THE ISUA SUPRACRUSTAL BELT

Non–plate tectonic models for the development of the Isua supracrustal belt are viable because the protolith lithologies at Isua are common to all >3.2 Ga greenstone belts, prograde amphibolite-grade metamorphism appears to be uniform across the belt, and pervasive sheath folding may have dominated the structural development. A simple interpretation for the assembly of the Isua supracrustal belt stratigraphy is that the ca. 3.7 Ga supracrustal rocks may have been deposited in sequence atop the ca. 3.8 Ga supracrustal rocks. This in turn allows a correspondingly simple structural model, in which all rocks older than the ca. 3.66–3.60 Ga granites have been flattened and stretched within sheath and curtain folds at outcrop to regional scales. Thus, the main stages of Eoarchean regional tectonic evolution would have proceeded as: (1) deposition of the ca. 3.8 Ga supracrustal sequence; (2) intrusion of the ca. 3.8 Ga supracrustal sequence by ca. 3.8 Ga TTGs (largely tonalitic); (3) deposition of the ca. 3.7 Ga supracrustal sequence; (4) intrusion of the ca. 3.7 Ga supracrustal sequence by ca. 3.7 Ga TTGs (largely tonalitic); and (5) amphibolite-facies metamorphism contemporaneous with regional flattening and stretching in sheath and curtain folds, likely within a larger shear zone, concluding with (or followed by) intrusion of ca. 3.66–3.60 Ga granite (Fig. 5).

In this model, crustal motion was dominated by vertical advection. For instance, both TTG bodies were intruded at roughly the same depth below the surface, but intrusion of similar TTG bodies at vertically separated crustal levels occurred because deposition of the ca. 3.7 Ga sequence and corresponding evacuation of underlying mantle source regions pushed down the older rocks, including the 3.8 Ga TTG body, relative to Earth's surface. This rapid downward advection also strongly limited burial metamorphism by rapid burial of cold (near-) surface temperatures, chilling the geotherm (cf. Moore and Webb, 2013). Thinning during the deformation event was dramatic: for example, the preserved portion of the ca. 3.7 Ga sequence, which now ranges from a few hundred meters up to ~2.7 km in thickness, would have been as thick as ~10 km prior to regional flattening. This is consistent with published outcrop-scale thinning estimates of 80%–90% (Fedo, 2000; Furnes et al., 2007).

DISCUSSION AND CONCLUSIONS

To address whether the Isua supracrustal belt is the single terrane older than 3.2 Ga requiring plate tectonics, as described in prior north- and south-dipping subduction models, or if it could also be viably interpreted via non–plate tectonic models, we (1) critically analyzed descriptions of published geochronology, focusing on U-Pb zircon age determinations and associated field relationships previously interpreted to reveal multiple episodes of plate-tectonic activity, and (2) conducted reconnaissance field-based examination of metamorphic and structural relationships across the belt. We found that: (1) Published field relationships with associated geochronological data proposed to record multiple distinct deformation events and differentiate them in time within the context of the north-dipping subduction model (e.g., Nutman et al., 2015b; Nutman and Friend, 2009) instead lack sufficient field and age constraints to uniquely support many of the claims. (2) Variable amounts of fluid flow resulting in a northeastward increase in the extent of retrograde metasomatism offer an alternative explanation for observations previously interpreted (Arai et al., 2015; Komiya et al., 1999) as a northeastward decrease in metamorphic grade and extrusion within the context of the south-dipping subduction model. (3) In contrast to strain concentrations via mylonitic shear zones and/or duplex systems predicted in plate-tectonic models, the strain may be quasi-uniform throughout the Isua supracrustal belt, with multiscale a-type folding extending even to the 10^4 m scale of the

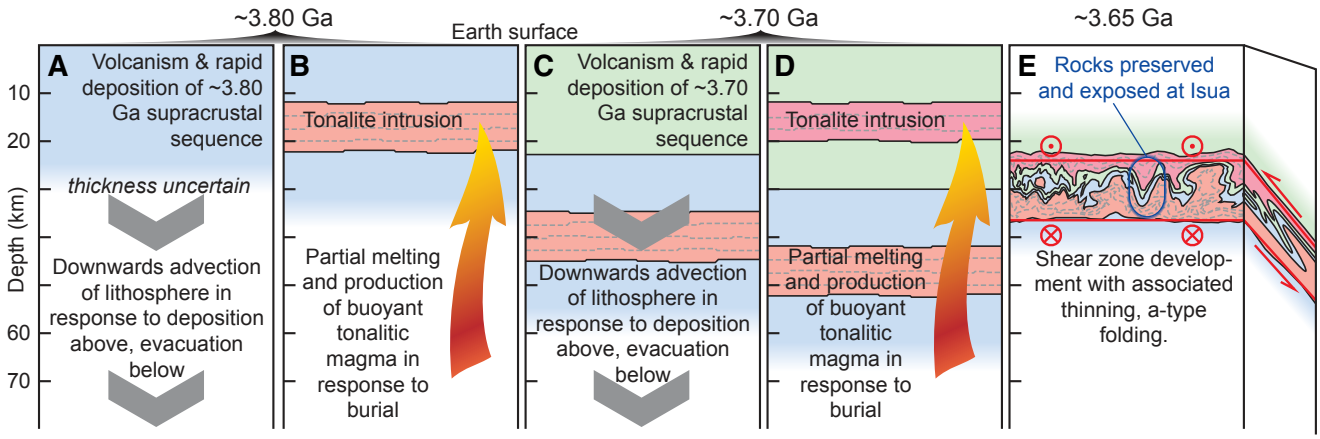

Figure 5. Vertical tectonics model for the Eoarchean development of the Isua supracrustal belt. (A) Rapid volcanism and concomitant burial of lithosphere composed largely of similar basaltic materials at ca. 3.80 Ga leads directly to (B) partial melting at depth, producing tonalitic melts that rise to intrude the ca. 3.80 Ga supracrustal sequence in sill geometries, forming large-scale ca. 3.80 Ga plutonic rocks. Second-order details and possibilities that are not shown include extrusive volcanism of some tonalitic melts to form felsic volcanic rocks, repeated volcanic and burial events within a time frame that appears unitary in the resolving power of U-Pb zircon geochronology, and the deposition of a relatively thin layer of sediment in the interim between 3.8 Ga and 3.7 Ga (which is later represented by the dividing sedimentary unit of Nutman et al., 2009). (C–D) Repetition of this cycle of volcanism, burial, and intrusion at ca. 3.70 Ga. The resultant post–3.7 Ga geometry features a layer-cake supracrustal/plutonic rock stratigraphy with ca. 3.7 Ga supracrustal rocks intruded by a layer dominated by ca. 3.7 Ga plutonic rocks stacked atop a similar set of ca. 3.8 Ga rocks. (E) This layer-cake stratigraphy is subjected to penetrative shearing and associated thinning within a shear zone, here speculated to be contractional. The quasi-uniform strain recorded across the supracrustal belt reflects a preserved fragment of an a-type fold system within the postulated shear zone. The geometry of the a-type folding shown here is inspired by detailed three-dimensional analysis by Wex et al. (2014) of a natural example of such structures. The extent of thinning is consistent with published estimates from outcrop-scale analyses (Fedo, 2000; Furnes et al., 2007).

entire warped belt. The Isua supracrustal belt can therefore be viably interpreted as Earth's largest known exposed a-type fold. On the bases of these findings, we propose a new tectonic model involving two cycles of volcanism and burial resulting in melting and TTG intrusion, which collectively produced the supracrustal belt protoliths and adjacent TTG bodies, followed by a major shear event, which produced the Isua a-type folding.

A series of implications for early Earth development follows from this new model. First, because the Isua supracrustal belt can be interpreted via vertical stacking without a suture zone, dominantly horizontal/plate tectonics are not required to understand any terranes older than 3.2 Ga. The regional tectonic event prior to 3.66–3.60 Ga granitic intrusion, which featured amphibolite-facies metamorphism and dramatic deformation, could be interpreted in plate-tectonic context. However, vertical tectonics can also create large-scale crustal deformations in response to radial constriction, such as the ~20-km-high mountains developing on Jupiter's volcanic moon Io, i.e., the solar system's example of active heat-pipe vertical tectonics (e.g., McKinnon et al., 2001). It follows that Earth may not have experienced plate tectonics for the first third of its history. Second, the Isua record suggests faster downward vertical advection of crust at ca. 3.8–3.7 Ga as contrasted to rates at the similar ca. 3.55–3.2 Ga Barberton and Pilbara greenstone belts of South Africa and Australia, respectively. This inference is drawn from the observation that the ca. 3.7 Ga TTG body at Isua was intruded into a higher portion of the crustal section versus the ca. 3.8 Ga TTG body, whereas at the younger terranes, TTG intrusions with similar temporal separation were intruded at the same crustal horizons (e.g., Van Kranendonk et al., 2007). If TTGs intruded at 3.8 Ga and 3.7 Ga at the same depth below an Earth surface of roughly constant elevation, the implied rate of lithospheric downward advection for this period is roughly 0.2 mm yr^{-1}, as calculated from the inferred thickness of the ca. 3.7 Ga supracrustal sequence versus the 100 m.y. interval (note that TTG bodies represent lithospheric melts [Moyen and Martin, 2012] and thus would not have contributed to overall lithospheric downward advection). Similar analyses of Barberton and Pilbara geology yielded lithospheric downward advection rates of 0.03, 0.07, and 0.12 mm yr^{-1} for the period of ca. 3.55–3.2 Ga at Barberton, the same period at Pilbara, and only the ca. 3.55–3.45 Ga period at Pilbara, respectively (Moore and Webb, 2013). Third, this slowdown of volcanism and corresponding lithospheric downward advection could have occurred gradually, or it may reflect a stepped transition associated with a rapid subduction catastrophe. Prior studies suggest that in such a scenario, mantle convective forcing would have overcome the strength of a single plate lithosphere, involving this lithosphere in the convection process (e.g., Kankanamge and Moore, 2016; Moore and Webb, 2013; Moresi and Solomatov, 1998). Once involved, a large fraction of the existing lithosphere would have rapidly subducted due to its weight and been replaced by juvenile lithosphere of sufficient youth and corresponding buoyancy to resist subduction, thereby temporarily reestablishing a single plate lithosphere (presumably cooling via hot stagnant lid, plume-dominated cooling, as described in Lenardic's [2018] classification scheme). Future work may examine possible tectonic evolutions, such as (1) if the Isua rocks represent the workings of an early single plate lithosphere exclusively, with the Eoarchean shearing representing an Io-analogous shortening event, or (2) if the deformation experienced at Isua between 3.7 Ga and 3.66–3.60 Ga records a crustal response to a subduction episode, and the Barberton and Pilbara greenstone belts reflect the renewed, slower development of a single plate lithosphere.

The pulses of high-volume volcanism implied by the new model appear dramatically nonuniformitarian and thus difficult to visualize. The model involves deposition of over 25 km of mafic and felsic volcanic rocks in a brief period (up to ~10 m.y.?), followed by ~100 m.y. of quiescence, and then a similar pulse of volcanism. Comparisons to the geologies of Io, Barberton, and Pilbara offer a degree of reassurance. Io is observed to deposit new volcanic material at a globally averaged rate of roughly a centimeter per year (O'Reilly and Davies, 1981; Carr et al., 1998), i.e., dramatically faster than the 0.2 mm yr^{-1} rate indicated for Isua by the new model. Nonetheless, even at Io, there are clear periods of quiescence, as the surface shows an anticorrelation of volcanic centers with mountain belts (McKinnon et al., 2001). The somewhat slower rates of volcanic resurfacing observed at Barberton and Pilbara were accomplished in similar pulses, with intervening periods of quiescence ranging from roughly 30 to 100 m.y. (e.g., Van Kranendonk et al., 2007; Byerly et al., 2019). Therefore, the proposed Isua volcanism is consistent with observed patterns. The distinct rates differentiating Isua from Barberton and Pilbara imply that Earth's mantle was warmer at ca. 3.8–3.7 Ga versus ca. 3.5–3.2 Ga, which seems a reasonable inference given decaying radioactive heat sources.

This work fits within the larger context of growing awareness that terrestrial bodies in our solar system, and likely beyond, have experienced similar early evolutions: from magma oceans to heat-pipe single plate cooling, followed in most cases by transitions to plate-tectonic, stagnant lid, and/or episodic overturn cooling (Beall et al., 2018; Moore et al., 2017; Ricard et al., 2014). This new understanding of the evolution of the Isua supracrustal belt, together with established knowledge about the Barberton and Pilbara greenstone belts, indicates that Earth experienced either heat-pipe cooling or episodic overturn cooling during the Eoarchean and Paleoarchean. It follows that study of early Earth terranes can be considered increasingly useful for comparative planetology, both in terms of records of crust-mantle interaction and astrobiology—and such exploration is cost-effective versus rovers.

ACKNOWLEDGMENTS

We thank Julie Hollis and the Greenland Ministry of Mineral Resources, Air Greenland, and Blue Water Greenland A/S for logistical support. This research was supported by the University of Hong Kong via: (1) start-up funds (to Webb) and (2) Seed Fund for Basic Research 104004325 (to Webb and Müller). Thoughtful reviews from Hugh Rollinson and an anonymous reviewer are gratefully acknowledged for their contributions to improving the manuscript; all mistakes are our own.

REFERENCES CITED

Allwood, A.C., Rosing, M.T., Flannery, D.T., Hurowitz, J.A., and Heirwegh, C.M., 2018, Reassessing evidence of life in 3,700-million-year-old rocks of Greenland: Nature, v. 563, no. 7730, p. 241, https://doi.org/10.1038/s41586-018-0610-4.

Alsop, G.I., and Holdsworth, R.E., 2012, The three dimensional shape and localisation of deformation within multilayer sheath folds: Journal of Structural Geology, v. 44, p. 110–128, https://doi.org/10.1016/j.jsg.2012.08.015.

Appel, P.W.U., Fedo, C.M., Moorbath, S., and Myers, J.S., 1998, Recognizable primary volcanic and sedimentary features in a low-strain domain of the highly deformed, oldest known (approximate to 3.7–3.8 Gyr) greenstone belt, Isua, West Greenland: Terra Nova, v. 10, no. 2, p. 57–62, https://doi.org/10.1046/j.1365-3121.1998.00162.x.

Arai, T., Omori, S., Komiya, T., and Maruyama, S., 2015, Intermediate *P*/*T*-type regional metamorphism of the Isua supracrustal belt, southern West Greenland: The oldest Pacific-type orogenic belt?: Tectonophysics, v. 662, p. 22–39, https://doi.org/10.1016/j.tecto.2015.05.020.

Beall, A.P., Moresi, L., and Cooper, C.M., 2018, Formation of cratonic lithosphere during the initiation of plate tectonics: Geology, v. 46, no. 6, p. 487–490, https://doi.org/10.1130/G39943.1.

Bédard, J.H., Brouillette, P., Madore, L., and Berclaz, A., 2003, Archaean cratonization and deformation in the northern Superior Province, Canada: An evaluation of plate tectonic versus vertical tectonic models: Precambrian Research, v. 127, no. 1–3, p. 61–87, https://doi.org/10.1016/S0301-9268(03)00181-5.

Bennett, V.C., Brandon, A.D., and Nutman, A.P., 2007, Coupled Nd-142–Nd-143 isotopic evidence for Hadean mantle dynamics: Science, v. 318, no. 5858, p. 1907–1910, https://doi.org/10.1126/science.1145928.

Bird, P., Liu, Z., and Rucker, W.K., 2008, Stresses that drive the plates from below: Definitions, computational path, model optimization, and error analysis: Journal of Geophysical Research–Solid Earth, v. 113, no. B11, B11406, https://doi.org/10.1029/2007JB005460.

Blichert-Toft, J., and Frei, R., 2001, Complex Sm-Nd and Lu-Hf isotope systematics in metamorphic garnets from the Isua supracrustal belt, West Greenland: Geochimica et Cosmochimica Acta, v. 65, p. 3177–3189, https://doi.org/10.1016/S0016-7037(01)00680-9.

Boos, W.R., and Kuang, Z., 2010, Dominant control of the South Asian monsoon by orographic insulation versus

plateau heating: Nature, v. 463, no. 7278, p. 218–222, https://doi.org/10.1038/nature08707.
Bowring, S.A., and Williams, I.S., 1999, Priscoan (4.00–4.03 Ga) orthogneisses from northwestern Canada: Contributions to Mineralogy and Petrology, v. 134, no. 1, p. 3–16, https://doi.org/10.1007/s004100050465.
Bridgwater, D., and McGregor, V. R., 1974, Field work on the very early Precambrian rocks of the Isua area, southern West Greenland: Grønlands Geologiske Undersøgelse Rapport 65, p. 49–54.
Brown, M., and Johnson, T., 2018, Secular change in metamorphism and the onset of global plate tectonics: The American Mineralogist, v. 103, no. 2, p. 181–196, https://doi.org/10.2138/am-2018-6166.
Byerly, G.R., Lowe, D.R., and Heubeck, C., 2019, Geologic evolution of the Barberton greenstone belt—A unique record of crustal development, surface processes, and early life, *in* Van Kranendonk, M.J., Bennett, V.C., and Hoffmann, J.E., eds., Earth's Oldest Rocks (2nd ed.): Amsterdam, Elsevier, p. 569–613, https://doi.org/10.1016/B978-0-444-63901-1.00024-1.
Cabral, R.A., Jackson, M.G., Rose-Koga, E.F., Koga, K.T., Whitehouse, M.J., Antonelli, M.A., Farquhar, J., Day, J.M.D., and Hauri, E.H., 2013, Anomalous sulphur isotopes in plume lavas reveal deep mantle storage of Archaean crust: Nature, v. 496, no. 7446, p. 490–493, https://doi.org/10.1038/nature12020.
Caro, G., Bourdon, B., Birck, J.L., and Moorbath, S., 2003, ^{146}Sm-^{142}Nd evidence from Isua metamorphosed sediments for early differentiation of the Earth's mantle: Nature, v. 423, p. 428–432, https://doi.org/10.1038/nature01668.
Carr, M.H., McEwan, A.S., Howard, K.A., Chuang, F.C., Thomas, P., Schuster, P., Oberst, J., Neukum, G., Schubert, G., and the Galileo Imaging Team, 1998, Mountains and calderas on Io: Possible implications for lithosphere structure and magma generation: Icarus, v. 135, p. 146–165.
Cates, N.L., Ziegler, K., Schmitt, A.K., and Mojzsis, S.J., 2013, Reduced, reused and recycled: Detrital zircons define a maximum age for the Eoarchean (ca. 3750–3780 Ma) Nuvvuagittuq supracrustal belt, Quebec (Canada): Earth and Planetary Science Letters, v. 362, p. 283–293, https://doi.org/10.1016/j.epsl.2012.11.054.
Chemenda, A.I., Mattauer, M., Malavieille, J., and Bokun, A.N., 1995, A mechanism for syncollisional rock exhumation and associated normal faulting—Results from physical modeling: Earth and Planetary Science Letters, v. 132, no. 1–4, p. 225–232, https://doi.org/10.1016/0012-821X(95)00042-B.
Cobbold, P.R., and Quinquis, H., 1980, Development of sheath folds in shear regimes: Journal of Structural Geology, v. 2, no. 1–2, p. 119–126, https://doi.org/10.1016/0191-8141(80)90041-3.
Compston, W., and Pidgeon, R.T., 1986, Jack Hills, evidence of more very old detrital zircons in Western Australia: Nature, v. 321, no. 6072, p. 766–769, https://doi.org/10.1038/321766a0.
Condie, K., 2003, Incompatible element ratios in oceanic basalts and komatiites: Tracking deep mantle sources and continental growth rates with time: Geochemistry Geophysics Geosystems, v. 4, p. 1–28, https://doi.org/10.1029/2002GC000333.
Condie, K., 2015, Changing tectonic settings through time: Indiscriminate use of geochemical discriminant diagrams: Precambrian Research, v. 266, p. 587–591, https://doi.org/10.1016/j.precamres.2015.05.004.
Condie, K., 2019, Earth's oldest rocks and minerals, *in* Van Kranendonk, M.J., Bennett, V.C., and Hoffmann, J.E., eds., Earth's Oldest Rocks (2nd ed.): Amsterdam, Elsevier, p. 239–253, https://doi.org/10.1016/B978-0-444-63901-1.00011-3.
Crowe, S.A., Dossing, L.N., Beukes, N.J., Bau, M., Kruger, S.J., Frei, R., and Canfield, D.E., 2013, Atmospheric oxygenation three billion years ago: Nature, v. 501, no. 7468, p. 535–538, https://doi.org/10.1038/nature12426.
Crowley, J.L., 2003, U-Pb geochronology of 3810–3630 Ma granitoid rocks south of the Isua greenstone belt, southern West Greenland: Precambrian Research, v. 126, no. 3–4, p. 235–257.
Crowley, J.L., Myers, J.S., and Dunning, G.R., 2002, Timing and nature of multiple 3700–3600 Ma tectonic events in intrusive rocks north of the Isua greenstone belt, southern West Greenland: Geological Society of America Bulletin, v. 114, no. 10, p. 1311–1325, https://doi.org/10.1130/0016-7606(2002)114<1311:TANOMM>2.0.CO;2.
Davaille, A., Smrekar, S.E., and Tomlinson, S., 2017, Experimental and observational evidence for plume-induced subduction on Venus: Nature Geoscience, v. 10, p. 349–355, https://doi.org/10.1038/ngeo2928.
Dhuime, B., Hawkesworth, C.J., Cawood, P.A., and Storey, C.D., 2012, A change in the geodynamics of continental growth 3 billion years ago: Science, v. 335, no. 6074, p. 1334–1336, https://doi.org/10.1126/science.1216066.
Faure, G., 1986, Principles of Isotope Geology: New York, Wiley, 589 p.
Fedo, C.M., 2000, Setting and origin for problematic rocks from the >3.7 Ga Isua greenstone belt, southern West Greenland: Earth's oldest coarse clastic sediments: Precambrian Research, v. 101, no. 1, p. 69–78.
Fedo, C.M., Myers, J.S., and Appel, P.W.U., 2001, Depositional setting and paleogeographic implications of Earth's oldest supracrustal rocks, the >3.7 Ga Isua greenstone belt, West Greenland: Sedimentary Geology, v. 141, p. 61–77, https://doi.org/10.1016/S0037-0738(01)00068-9.
Fisher, C.M., and Vervoort, J.D., 2018, Using the magmatic record to constrain the growth of continental crust—The Eoarchean zircon Hf record of Greenland: Earth and Planetary Science Letters, v. 488, p. 79–91, https://doi.org/10.1016/j.epsl.2018.01.031.
Frei, R., Rosing, M.T., Waight, T.E., and Ulfbeck, D.G., 2002, Hydrothermal-metasomatic and tectono-metamorphic processes in the Isua supracrustal belt (West Greenland): A multi-isotopic investigation of their effects on the Earth's oldest oceanic crustal sequence: Geochimica et Cosmochimica Acta, v. 66, p. 467–486, https://doi.org/10.1016/S0016-7037(01)00781-5.
Frei, R., Crowe, S.A., Bau, M., Polat, A., Fowle, D.A., and Dossing, L.N., 2016, Oxidative elemental cycling under the low O_2 Eoarchean atmosphere: Scientific Reports, v. 6, p. 21058, https://doi.org/10.1038/srep21058.
Friend, C.R.L., and Nutman, A.P., 2005, Complex 3670–3500 Ma orogenic episodes superimposed on juvenile crust accreted between 3850 and 3690 Ma, Itsaq Gneiss Complex, southern West Greenland: The Journal of Geology, v. 113, no. 4, p. 375–397, https://doi.org/10.1086/430239.
Friend, C.R.L., and Nutman, A.P., 2010, Eoarchean ophiolites? New evidence for the debate on the Isua supracrustal belt, southern West Greenland: American Journal of Science, v. 310, no. 9, p. 826–861, https://doi.org/10.2475/09.2010.04.
Friend, C.R.L., and Nutman, A.P., 2011, Dunites from Isua, Greenland: A ca. 3720 Ma window into subcrustal metasomatism of depleted mantle: Geology, v. 39, no. 7, p. 663–666, https://doi.org/10.1130/G31904.1.
Friend, C.R.L., Bennett, V.C., and Nutman, A.P., 2002, Abyssal peridotites >3,800 Ma from southern West Greenland: Field relationships, petrography, geochronology, whole-rock and mineral chemistry of dunite and harzburgite inclusions in the Itsaq Gneiss Complex: Contributions to Mineralogy and Petrology, v. 143, no. 1, p. 71–92, https://doi.org/10.1007/s00410-001-0332-7.
Friend, C.R.L., Nutman, A.P., Bennett, V.C., and Norman, M.D., 2008, Seawater-like trace element signatures (REE+Y) of Eoarchaean chemical sedimentary rocks from southern West Greenland, and their corruption during high-grade metamorphism: Contributions to Mineralogy and Petrology, v. 155, no. 2, p. 229–246, https://doi.org/10.1007/s00410-007-0239-z.
Froude, D.O., Ireland, T.R., Kinny, P.D., Williams, I.S., Compston, W., Williams, I.R., and Myers, J.S., 1983, Ion microprobe identification of 4,100–4,200 Myr-old terrestrial zircons: Nature, v. 304, no. 5927, p. 616–618, https://doi.org/10.1038/304616a0.
Furnes, H., de Wit, M., Staudigel, H., Rosing, M., and Muehlenbachs, K., 2007, A vestige of Earth's oldest ophiolite: Science, v. 315, no. 5819, p. 1704–1707, https://doi.org/10.1126/science.1139170.
Gardiner, N.J., Johnson, T.E., Kirkland, C.L., and Szilas, K., 2019, Modelling the hafnium-neodymium evolution of early Earth: A study of West Greenland: Journal of Petrology, v. 60, p. 177–197, https://doi.org/10.1093/petrology/egy110.
Hanmer, S., and Greene, D.C., 2002, A modern structural regime in the Paleoarchean (~3.64 Ga); Isua greenstone belt, southern West Greenland: Tectonophysics, v. 346, no. 3, p. 201–222, https://doi.org/10.1016/S0040-1951(02)00029-X.
Hanmer, S., Hamilton, M.A., and Crowley, J.L., 2002, Geochronological constraints on Paleoarchean thrust-nappe and Neoarchean accretionary tectonics in southern West Greenland: Tectonophysics, v. 350, no. 3, p. 255–271, https://doi.org/10.1016/S0040-1951(02)00120-8.
Harrison, T.M., Bell, E.A., and Boehnke, P., 2017, Hadean Zircon Petrochronology: Mineralogical Society of America Volume 83: Petrochronology: Methods and Applications, 329 p.
Hassenkam, T., Andersson, M.P., Dalby, K.N., Mackenzie, D.M.A., and Rosing, M.T., 2017, Elements of Eoarchean life trapped in mineral inclusions: Nature, v. 548, no. 7665, p. 78–81, https://doi.org/10.1038/nature23261.
Hayashi, M., Komiya, T., Nakamura, Y., and Maruyama, S., 2000, Archean regional metamorphism of the Isua supracrustal belt, southern West Greenland: Implications for a driving force for Archean plate tectonics: International Geology Review, v. 42, no. 12, p. 1055–1115, https://doi.org/10.1080/00206810009465128.
Hazen, R.M., Papineau, D., Leeker, W.B., Downs, R.T., Ferry, J.M., McCoy, T.J., Sverjensky, D.A., and Yang, H.X., 2008, Mineral evolution: The American Mineralogist, v. 93, no. 11–12, p. 1693–1720, https://doi.org/10.2138/am.2008.2955.
Herman, F., Seward, D., Valla, P.G., Carter, A., Kohn, B., Willett, S.D., and Ehlers, T.A., 2013, Worldwide acceleration of mountain erosion under a cooling climate: Nature, v. 504, no. 7480, p. 423–426, https://doi.org/10.1038/nature12877.
Hoffmann, J.E., Nagel, T.J., Münker, C., Næraa, T., and Rosing, M.T., 2014, Constraining the process of Eoarchean TTG formation in the Itsaq Gneiss Complex, southern West Greenland: Earth and Planetary Science Letters, v. 388, p. 374–386, https://doi.org/10.1016/j.epsl.2013.11.050.
Hoorn, C., Wesselingh, F.P., ter Steege, H., Bermudez, M.A., Mora, A., Sevink, J., Sanmartin, I., Sanchez-Meseguer, A., Anderson, C.L., Figueiredo, J.P., Jaramillo, C., Riff, D., Negri, F.R., Hooghiemstra, H., Lundberg, J., Stadler, T., Sarkinen, T., and Antonelli, A., 2010, Amazonia through time: Andean uplift, climate change, landscape evolution, and biodiversity: Science, v. 330, no. 6006, p. 927–931, https://doi.org/10.1126/science.1194585.
Huntington, K.W., and Klepeis, K.A., 2018, Challenges and Opportunities for Research in Tectonics: Understanding Deformation and the Processes that Link Earth Systems, from Geologic Time to Human Time: A community vision document submitted to the U.S. National Science Foundation: Washington, D.C., ResearchWorks Archive, 84 p., http://hdl.handle.net/1773/40754.
Inger, S., and Harris, N., 1993, Geochemical constraints on leucogranite magmatism in the Langtang Valley, Nepal Himalaya: Journal of Petrology, v. 34, no. 2, p. 345–368, https://doi.org/10.1093/petrology/34.2.345.
James, P.R., 1976, Deformation of Isua block, West Greenland—Remnant of earliest stable continental crust: Canadian Journal of Earth Sciences, v. 13, no. 6, p. 816–823, https://doi.org/10.1139/e76-084.
Johnson, I.E., Kirkland, C.L., Gardiner, N.J., Brown, M., Smithies, R.H., and Santosh, M., 2019, Secular change in TTG compositions: Implications for the evolution of Archaean geodynamics: Earth and Planetary Science Letters, v. 505, p. 65–75, https://doi.org/10.1016/j.epsl.2018.10.022.
Kaczmarek, M.A., Reddy, S.M., Nutman, A.P., Friend, C.R.L., and Bennett, V.C., 2016, Earth's oldest mantle fabrics indicate Eoarchaean subduction: Nature Communications, v. 7, p. 10665, https://doi.org/10.1038/ncomms10665.
Kamber, B.S., Whitehouse, M.J., Bolhar, R., and Moorbath, S., 2005, Volcanic resurfacing and the early terrestrial crust: Zircon U-Pb and REE constraints from the Isua greenstone belt, southern West Greenland: Earth and Planetary Science Letters, v. 240, no. 2, p. 276–290, https://doi.org/10.1016/j.epsl.2005.09.037.
Kankanamge, D.G.J., and Moore, W.B., 2016, Heat transport in the Hadean mantle: From heat pipes to plates: Geophysical Research Letters, v. 43, no. 7, p. 3208–3214, https://doi.org/10.1002/2015GL067411.
Keller, C.B., and Schoene, B., 2012, Statistical geochemistry reveals disruption in secular lithospheric evolution about 2.5 Gyr ago: Nature, v. 485, p. 490–493, https://doi.org/10.1038/nature11024.

Keto, L., and Kurki, J., 1967, Report on the Exploration Activity at Isua: Geological Survey of Denmark and Greenland Report 20024.

Komiya, T., Maruyama, S., Masuda, T., Nohda, S., Hayashi, M., and Okamoto, K., 1999, Plate tectonics at 3.8–3.7 Ga: Field evidence from the Isua accretionary complex, southern West Greenland: The Journal of Geology, v. 107, no. 5, p. 515–554, https://doi.org/10.1086/314371.

Kurki, J., and Keto, L., 1966, Report on Geological Investigations at Isua: Geological Survey of Denmark and Greenland Report 20219.

Lenardic, A., 2018, The diversity of tectonic modes and thoughts about transitions between them: Philosophical Transactions of the Royal Society, ser. A, Mathematical, Physical and Engineering Sciences, v. 376, no. 2132, 20170416, https://doi.org/10.1098/rsta.2017.0416.

Ludwig, K.R., 2012, User's Manual for Isoplot 3.75: A Geochronological Toolkit for Microsoft Excel: Berkeley Geochronology Center Special Publication 5, 75 p.

McKenzie, N.R., Horton, B.K., Loomis, S.E., Stockli, D.F., Planavsky, N.J., and Lee, C.T.A., 2016, Continental arc volcanism as the principal driver of icehouse-greenhouse variability: Science, v. 352, no. 6284, p. 444–447, https://doi.org/10.1126/science.aad5787.

McKinnon, W.B., Schenk, P.M., and Dombard, A.J., 2001, Chaos on Io: A model for formation of mountain blocks by crustal heating, melting, and tilting: Geology, v. 29, no. 2, p. 103–106, https://doi.org/10.1130/0091-7613(2001)029<0103:COIAMF>2.0.CO;2.

Michalski, J.R., Onstott, T.C., Mojzsis, S.J., Mustard, J., Chan, Q.H.S., Niles, P.B., and Johnson, S.S., 2018, The Martian subsurface as a potential window into the origin of life: Nature Geoscience, v. 11, no. 1, p. 21–26, https://doi.org/10.1038/s41561-017-0015-2.

Mojzsis, S.J., Harrison, T.M., and Pidgeon, R.T., 2001, Oxygen-isotope evidence from ancient zircons for liquid water at the Earth's surface 4,300 Myr ago: Nature, v. 409, no. 6817, p. 178–181, https://doi.org/10.1038/35051557.

Moorbath, S., O'Nions, R.K., Pankhurst, R.J., Gale, N.H., and McGregor, V.R., 1972, Further rubidium-strontium age determinations on the very early Precambrian rocks of the Godthaab district, West Greenland: Nature, v. 240, p. 78–82.

Moorbath, S., Onions, R.K., and Pankhurst, R.J., 1973, Early Archaean age for Isua iron formation, West Greenland: Nature, v. 245, no. 5421, p. 138–139, https://doi.org/10.1038/245138a0.

Moore, W.B., and Webb, A.A.G., 2013, Heat-pipe Earth: Nature, v. 501, no. 7468, p. 501–505, https://doi.org/10.1038/nature12473.

Moore, W.B., Simon, J.I., and Webb, A.A.G., 2017, Heat-pipe planets: Earth and Planetary Science Letters, v. 474, p. 13–19, https://doi.org/10.1016/j.epsl.2017.06.015.

Moresi, L., and Solomatov, V., 1998, Mantle convection with a brittle lithosphere: Thoughts on the global tectonic styles of the Earth and Venus: Geophysical Journal International, v. 133, no. 3, p. 669–682, https://doi.org/10.1046/j.1365-246X.1998.00521.x.

Moyen, J.F., and Martin, H., 2012, Forty years of TTG research: Lithos, v. 148, p. 312–336, https://doi.org/10.1016/j.lithos.2012.06.010.

Myers, J.S., 2001, Protoliths of the 3.8–3.7 Ga Isua greenstone belt, West Greenland: Precambrian Research, v. 105, no. 2–4, p. 129–141, https://doi.org/10.1016/S0301-9268(00)00108-X.

Næraa, T., Schersten, A., Rosing, M.T., Kemp, A.I.S., Hoffmann, J.E., Kokfelt, T.F., and Whitehouse, M.J., 2012, Hafnium isotope evidence for a transition in the dynamics of continental growth 3.2Gyr ago: Nature, v. 485, no. 7400, p. 627–630, https://doi.org/10.1038/nature11140.

Nutman, A.P., 1984, Early Archaean crustal evolution of the Isukasia area, southern West Greenland, *in* Kröner, A., and Greiling, R., eds., Precambrian Tectonics Illustrated: Stuttgart, Germany, E. Schweizerbart'sche Verlagsbuchhandlung (Nagele u. Obermiller), p. 79–93.

Nutman, A.P., and Bennett, V.C., 2019, The 3.9–3.6 Ga Itsaq Gneiss Complex of Greenland, *in* van Kranendonk, M.J., Bennett, V.C., and Hoffmann, J.E., eds., Earth's Oldest Rocks (2nd ed.): Amsterdam, Elsevier, p. 375–399.

Nutman, A.P., and Bridgwater, D., 1986, Early Archean Amitsoq tonalites and granites of the Isukasia area, southern West Greenland—Development of the oldest-known sial: Contributions to Mineralogy and Petrology, v. 94, no. 2, p. 137–148, https://doi.org/10.1007/BF00592931.

Nutman, A.P., and Collerson, K.D., 1991, Very early Archean crustal-accretion complexes preserved in the North Atlantic craton: Geology, v. 19, no. 8, p. 791–794, https://doi.org/10.1130/0091-7613(1991)019<0791:VEACAC>2.3.CO;2.

Nutman, A.P., and Friend, C.R.L., 2007, Comment on "A vestige of Earth's oldest ophiolite": Science, v. 318, no. 5851, p. 746, https://doi.org/10.1126/science.1144148.

Nutman, A.P., and Friend, C.R.L., 2009, New 1:20,000 scale geological maps, synthesis and history of investigation of the Isua supracrustal belt and adjacent orthogneisses, southern West Greenland: A glimpse of Eoarchaean crust formation and orogeny: Precambrian Research, v. 172, no. 3–4, p. 189–211, https://doi.org/10.1016/j.precamres.2009.03.017.

Nutman, A.P., McGregor, V.R., Friend, C.R.L., Bennett, V.C., and Kinny, P.D., 1996, The Itsaq Gneiss Complex of southern west Greenland: The world's most extensive record of early crustal evolution (3900–3600 Ma): Precambrian Research, v. 78, no. 1–3, p. 1–39, https://doi.org/10.1016/0301-9268(95)00066-6.

Nutman, A.P., Bennett, V.C., Friend, C.R.L., and Rosing, M.T., 1997, ~3710 and ≥3790 Ma volcanic sequences in the Isua (Greenland) supracrustal belt; structural and Nd isotope implications: Chemical Geology, v. 141, no. 3–4, p. 271–287, https://doi.org/10.1016/S0009-2541(97)00084-3.

Nutman, A.P., Bennett, V.C., Friend, C.R.L., and McGregor, V.R., 2000, The early Archaean Itsaq Gneiss Complex of southern West Greenland: The importance of field observations in interpreting age and isotopic constraints for early terrestrial evolution: Geochimica et Cosmochimica Acta, v. 64, no. 17, p. 3035–3060, https://doi.org/10.1016/S0016-7037(99)00431-7.

Nutman, A.P., Friend, C.R.L., and Bennett, V.C., 2002, Evidence for 3650–3600 Ma assembly of the northern end of the Itsaq Gneiss Complex, Greenland: Implication for early Archaean tectonics: Tectonics, v. 21, no. 1, p. 5-1–5-28, https://doi.org/10.1029/2000TC001203.

Nutman, A.P., Friend, C.R.L., Bennett, V.C., and McGregor, V.R., 2004, Dating of the Ameralik dyke swarms of the Nuuk district, southern West Greenland: Mafic intrusion events starting from c. 3510 Ma: Journal of the Geological Society [London], v. 161, p. 421–430, https://doi.org/10.1144/0016-764903-043.

Nutman, A.P., Friend, C.R.L., Horie, K., and Hidaka, H., 2007, The Itsaq Gneiss Complex of southern West Greenland and the construction of Eoarchaean crust at convergent plate boundaries, *in* Van Kranendonk, M.J., Smithies, R.H., and Bennett, V.C., eds., Earth's Oldest Rocks: Amsterdam, Elsevier, Developments in Precambrian Geology 15, p. 187–218, https://doi.org/10.1016/S0166-2635(07)15033-7.

Nutman, A.P., Friend, C.R.L., and Paxton, S., 2009, Detrital zircon sedimentary provenance ages for the Eoarchaean Isua supracrustal belt southern West Greenland: Juxtaposition of an imbricated ca. 3700 Ma juvenile arc against an older complex with 3920–3760 Ma components: Precambrian Research, v. 172, no. 3–4, p. 212–233, https://doi.org/10.1016/j.precamres.2009.03.019.

Nutman, A.P., Friend, C.R.L., Bennett, V.C., Wright, D., and Norman, M.D., 2010, >= 3700 Ma pre-metamorphic dolomite formed by microbial mediation in the Isua supracrustal belt (W. Greenland): Simple evidence for early life?: Precambrian Research, v. 183, no. 4, p. 725–737, https://doi.org/10.1016/j.precamres.2010.08.006.

Nutman, A.P., Bennett, V.C., Friend, C.R.L., Hidaka, H., Yi, K., Lee, S.R., and Kamiichi, T., 2013, The Itsaq Gneiss Complex of Greenland: Episodic 3900 to 3660 Ma juvenile crust formation and recycling in the 3660 to 3600 Ma Isukasian orogeny: American Journal of Science, v. 313, no. 9, p. 877–911, https://doi.org/10.2475/09.2013.03.

Nutman, A.P., Bennett, V.C., Chivas, A.R., Friend, C.R.L., Liu, X.M., and Dux, F.W., 2015a, 3806 Ma Isua rhyolites and dacites affected by low temperature Eoarchaean surficial alteration: Earth's earliest weathering: Precambrian Research, v. 268, p. 323–338, https://doi.org/10.1016/j.precamres.2015.07.014.

Nutman, A.P., Bennett, V.C., and Friend, C.R.L., 2015b, The emergence of the Eoarchaean proto-arc: Evolution of a c. 3700 Ma convergent plate boundary at Isua, southern West Greenland, *in* Roberts, N.M.W., Van Kranendonk, M.J., Parman, S., Shirey, S., and Clift, P.D., eds., Continent Formation Through Time: The Geological Society [London] Special Publications 389, p. 113–133, https://doi.org/10.1144/SP389.5.

Nutman, A.P., Bennett, V.C., and Friend, C.R.L., 2015c, Proposal for a continent 'Itsaqia' amalgamated at 3.66 Ga and rifted apart from 3.53 Ga: Initiation of a Wilson cycle near the start of the rock record: American Journal of Science, v. 315, no. 6, p. 509–536, https://doi.org/10.2475/06.2015.01.

Nutman, A.P., Bennett, V.C., Friend, C.R.L., Yi, K., and Lee, S.R., 2015d, Mesoarchaean collision of Kapisilik terrane 3070 Ma juvenile arc rocks and >3600 Ma Isukasia terrane continental crust (Greenland): Precambrian Research, v. 258, p. 146–160, https://doi.org/10.1016/j.precamres.2014.12.013.

Nutman, A.P., Bennett, V.C., Friend, C.R.L., Van Kranendonk, M.J., and Chivas, A.R., 2016, Rapid emergence of life shown by discovery of 3,700-million-year-old microbial structures: Nature, v. 537, no. 7621, p. 535–538, https://doi.org/10.1038/nature19355.

Nutman, A.P., Bennett, V.C., Friend, C.R.L., Van Kranendonk, M.J., Rothacker, L., and Chivas, A.R., 2019, Cross-examining Earth's oldest stromatolites: Seeing through the effects of heterogeneous deformation, metamorphism and metasomatism affecting Isua (Greenland) ~3700 Ma sedimentary rocks: Precambrian Research, v. 331, 105347, https://doi.org/10.1016/j.precamres.2019.105347.

O'Neil, J., Carlson, R.W., Francis, D., and Stevenson, R.K., 2008, Neodymium-142 evidence for Hadean mafic crust: Science, v. 321, no. 5897, p. 1828–1831, https://doi.org/10.1126/science.1161925.

O'Reilly, T.C., and Davies, G.F., 1981, Magma transport of heat on Io: A mechanism allowing a thick lithosphere: Geophysical Research Letters, v. 8, no. 4, p. 313–316.

Pease, V., Percival, J., Smithies, H., Stevens, G., and Van Kranendonk, M., 2008, When did plate tectonics begin? Evidence from the orogenic record, *in* Condie, K.C., and Pease, V., eds., When Did Plate Tectonics Begin on Planet Earth?: Geological Society of America Special Paper 440, p. 199–228, https://doi.org/10.1130/2008.2440(10).

Polat, A., and Hofmann, A.W., 2003, Alteration and geochemical patterns in the 3.7–3.8 Ga Isua greenstone belt, West Greenland: Precambrian Research, v. 126, no. 3–4, p. 197–218, https://doi.org/10.1016/S0301-9268(03)00095-0.

Polat, A., Hofmann, A.W., and Rosing, M.T., 2002, Boninite-like volcanic rocks in the 3.7–3.8 Ga Isua greenstone belt, West Greenland: Geochemical evidence for intra-oceanic subduction zone processes in the early Earth: Chemical Geology, v. 184, no. 3–4, p. 231–254, https://doi.org/10.1016/S0009-2541(01)00363-1.

Reimink, J.R., Davies, J.H.F.L., Chacko, T., Stern, R.A., Heaman, L.M., Sarkar, C., Schaltegger, U., Creaser, R.A., and Pearson, D.G., 2016, No evidence for Hadean continental crust within Earth's oldest evolved rock unit: Nature Geoscience, v. 9, no. 10, p. 777–780, https://doi.org/10.1038/ngeo2786.

Ricard, Y., Labrosse, S., and Dubuffet, F., 2014, Lifting the cover of the cauldron: Convection in hot planets: Geochemistry Geophysics Geosystems, v. 15, no. 12, p. 4617–4630, https://doi.org/10.1002/2014GC005556.

Rizo, H., Boyet, M., Blichert-Toft, J., O'Neil, J., Rosing, M.T., and Paquette, J.L., 2012, The elusive Hadean enriched reservoir revealed by Nd-142 deficits in Isua Archaean rocks: Nature, v. 491, no. 7422, p. 96–100, https://doi.org/10.1038/nature11565.

Rollinson, H., 2002, The metamorphic history of the Isua greenstone belt, West Greenland, *in* Fowler, C.M.R., Ebinger, C.J., and Hawkesworth, C.J., eds., The Early Earth: Physical, Chemical, and Biological Development: Geological Society [London] Special Publication 199, p. 329–350, https://doi.org/10.1144/GSL.SP.2002.199.01.16.

Rollinson, H., 2003, Metamorphic history suggested by garnet-growth chronologies in the Isua greenstone belt, West Greenland: Precambrian Research, v. 126, p. 181–196, https://doi.org/10.1016/S0301-9268(03)00094-9.

Rosing, M.T., Rose, N.M., Bridgwater, D., and Thomsen, H.S., 1996, Earliest part of Earth's stratigraphic record: A reappraisal of the >3.7 Ga Isua (Greenland) supracrustal sequence: Geology, v. 24, no. 1, p. 43–46, https://doi.org/10.1130/0091-7613(1996)024<0043:EPOESS>2.3.CO;2.

Rosing, M.T., Bird, D.K., Sleep, N.H., and Bjerrum, C.J., 2010, No climate paradox under the faint early Sun: Nature, v. 464, no. 7289, p. 744–747, https://doi.org/10.1038/nature08955.

Shirey, S.B., and Richardson, S.H., 2011, Start of the Wilson cycle at 3 Ga shown by diamonds from subcontinental mantle: Science, v. 333, no. 6041, p. 434–436, https://doi.org/10.1126/science.1206275.

Sleep, N.H., 2000, Evolution of the mode of convection within terrestrial planets: Journal of Geophysical Research–Planets, v. 105, no. E7, p. 17563–17578, https://doi.org/10.1029/2000JE001240.

Smithies, R.H., Van Kranendonk, M.J., and Champion, D.C., 2005, It started with a plume—Early Archaean basaltic proto-continental crust: Earth and Planetary Science Letters, v. 238, no. 3–4, p. 284–297, https://doi.org/10.1016/j.epsl.2005.07.023.

Stern, R.J., 2008, Modern-style plate tectonics began in Neoproterozoic time: An alternative interpretation of Earth's tectonic history, *in* Condie, K.C., and Pease, V., eds., When Did Plate Tectonics Begin on Planet Earth?: Geological Society of America Special Paper 440, p. 265–280, https://doi.org/10.1130/2008.2440(13).

Stern, R.J., Leybourne, M.I., and Tsujimori, T., 2016, Kimberlites and the start of plate tectonics: Geology, v. 44, no. 10, p. 799–802, https://doi.org/10.1130/G38024.1.

Szilas, K., Kelemen, P.B., and Rosing, M.T., 2015, The petrogenesis of ultramafic rocks in the > 3.7 Ga Isua supracrustal belt, southern West Greenland: Geochemical evidence for two distinct magmatic cumulate trends: Gondwana Research, v. 28, no. 2, p. 565–580, https://doi.org/10.1016/j.gr.2014.07.010.

Tang, M., Chen, K., and Rudnick, R.L., 2016, Archean upper crust transition from mafic to felsic marks the onset of plate tectonics: Science, v. 351, no. 6271, p. 372–375, https://doi.org/10.1126/science.aad5513.

Van Kranendonk, M.J., Smithies, R.H., Hickman, A.H., and Champion, D.C., 2007, Review: Secular tectonic evolution of Archean continental crust: Interplay between horizontal and vertical processes in the formation of the Pilbara craton, Australia: Terra Nova, v. 19, no. 1, p. 1–38, https://doi.org/10.1111/j.1365-3121.2006.00723.x.

Van Kranendonk, M.J., Smithies, R.H., and Champion, D.C., 2019, Paleoarchean development of a continental nucleus: The East Pilbara terrane of the Pilbara craton, Western Australia, *in* Van Kranendonk, M.J., Bennett, V.C., and Hoffmann, J.E., eds., Earth's Oldest Rocks (2nd ed.): Amsterdam, Elsevier, p. 437–462, https://doi.org/10.1016/B978-0-444-63901-1.00019-8.

Webb, A.A.G., Yin, A., Harrison, T.M., Celerier, J., Gehrels, G.E., Manning, C.E., and Grove, M., 2011, Cenozoic tectonic history of the Himachal Himalaya (northwestern India) and its constraints on the formation mechanism of the Himalayan orogen: Geosphere, v. 7, no. 4, p. 1013–1061, https://doi.org/10.1130/GES00627.1.

Wex, S., Passchier, C.W., de Kemp, E.A., and Ilhan, S., 2014, 3D visualization of sheath folds in Ancient Roman marble wall coverings from Ephesos, Turkey: Journal of Structural Geology, v. 67, p. 129–139, https://doi.org/10.1016/j.jsg.2014.07.005.

Wilde, S.A., Valley, J.W., Peck, W.H., and Graham, C.M., 2001, Evidence from detrital zircons for the existence of continental crust and oceans on the Earth 4.4 Gyr ago: Nature, v. 409, no. 6817, p. 175–178, https://doi.org/10.1038/35051550.

MANUSCRIPT RECEIVED 2 AUGUST 2019
REVISED MANUSCRIPT RECEIVED 18 DECEMBER 2019
MANUSCRIPT ACCEPTED 22 JANUARY 2020